FACULTY OF ENGINEERING AND TECHNOLOGY

DEPARTMENT OF WATER RESOURCES ENGINEERING

FINAL YEAR PROJECT

GEOTECHNICAL AND HYDRAULIC STABILITY ASSESSMENT OF RETAINING WALL FAILURES AT DOHO IRRIGATION SCHEME INTAKE FOR DESIGN IMPROVEMENT

CASE STUDY: BUTALEJA DISTRICT

BY

MUSIIMEGYE IVAN

(BU/UG/2022/1564)

SUPERVISOR

MR. KUSEMERERWA JOSEPH

A final year project submitted to the Department of Water Resources Engineering as a Partial fulfillment 0f the requirements for the award of a Bachelor of science in Water Resources Engineering of Busitema University.

APRIL - MAY 2026

ABSTRACT

The Doho Irrigation Scheme intake, a key structure supporting rice production in Eastern Uganda, has experienced retaining wall failures that threaten its operational reliability. This study assessed the geotechnical and hydraulic conditions at the intake to identify the governing failure mechanisms and develop practical design solutions. The methodology combined field soil sampling with laboratory tests, including shear strength and grain size analysis, and hydraulic evaluation of hydrostatic pressure, water currents, and scour effects. Stability analyses using Rankine and Coulomb earth pressure theories, supported by numerical modeling, showed that inadequate backfill drainage increased hydrostatic pressure, while toe scour reduced foundation support, resulting in factors of safety below the recommended 1.5. The study recommends installation of improved drainage provisions and enlargement of the wall base to enhance stability. These measures provide a practical basis for rehabilitating the intake and improving long-term reliability of water delivery within the scheme.

DECLARATION

I, MUSIIMEGYE IVAN, hereby declare that all the material presented in this project report is my original work and has not been previously submitted for the award of any degree, certificate, or diploma at any university or institution of higher learning.

Name: MUSIIMEGYE IVAN

Signature: ....

Date: 10\06|2026

APPROVAL

This is to certify that the project proposal under the title **"GEOTECHNICAL AND HYDRAULIC STABILITY ASSESSMENT OF RETAINING WALL FAILURES AT DOHO IRRIGATION SCHEME INTAKE FOR DESIGN IMPROVEMENT"** has been done under my guidance and supervision. The work presented in this report has been completed in accordance with the academic requirements of the university and is hereby approved for submission and examination.

Supervisor

Name: **Mr. Kusemererwa Joseph**

Busitema University Faculty of Engineering and Technology

Signature: ……………………………

Date: 10/JUN/2026

ACKNOWLEDGEMENT

I express my sincere gratitude to God Almighty for granting me good health, the gift of life, and the strength that enabled me to successfully conduct this research and compile the information presented in this report.

I am deeply grateful to my supervisor, **Mr. Kusemererwa Joseph**, for his invaluable guidance, continuous support, patience, and constructive advice throughout the implementation and completion of this study. His knowledge and professional insights greatly contributed to the successful completion of this work.

Also extend my appreciation to the staff of the Water Resources Engineering Department and the university at large for providing the academic environment and resources that facilitated the successful execution of this research.

Special appreciation is extended to my parents for their unwavering encouragement and financial support throughout my academic journey. Their dedication and sacrifices played a significant role in enabling the successful completion of this study.

Finally, I acknowledge my fellow students in the Water Resources class for their cooperation, encouragement, and sustained support during the implementation of this research.

TABLE OF CONTENTS

Table of Contents

LIST OF TABLES

LIST OF FIGURES

LIST OF ACRONYMS

DCP	Dynamic Cone Penetrometer.
FOS	Factor of Safety
SDG	Sustainable Development Goals
UNDP	United Nations Development Programme
LL	Liquid Limit
PL	Plastic Limit
LS	Linear Shrinkage
UNRA	Uganda National Roads Authority
GM	Grading Modulus
CC	Coefficient of Curvature
CU	Coefficient of Uniformity
SO	Specific Objective

1 CHAPTER ONE. INTRODUCTION.

This chapter is the general overview of the entire research study and it elaborates the background of the study, problem statement and objectives of the study, scope and justification of the study.

1.1 Background of the Study

Retaining wall failures are a global concern, often resulting from poor geotechnical design, Insufficient drainage, and lack of stability analysis. These failures can lead to landslides, infrastructure damage, and loss of life. A study by Kim (2025) emphasized that improper backfill, water pressure buildup, and insufficient reinforcement are common causes of wall instability. Hydraulic factors, such as seepage and poor water management, further exacerbate failure risks.(Kim, 2025)

In Africa, retaining wall failures are frequently linked to limited geotechnical investigations and poor hydraulic planning. Expansive soils, high rainfall, and Insufficient drainage systems contribute to instability. For example, in Nigeria and Kenya, infrastructure failures have been traced to poor soil characterization and lack of slope protection measures. Climate change has also intensified hydraulic loads, increasing the frequency of wall collapses.(Eze et al, 2024).

Uganda has experienced retaining wall failures in flood prone areas such as Kampala and Entebbe. Rising water levels in Lake Victoria have damaged embankments and retaining structures, revealing faults in hydraulic design and soil stabilization. The Uganda National Roads Authority (UNRA) has highlighted the need for integrated geotechnical and hydrological assessments in infrastructure planning.(Pietroiusti et al, 2023).

The Doho Irrigation Scheme which covers 2500 acres, located in Butaleja District, Eastern Uganda, is a key rice-growing area. The intake structure relies on retaining walls to manage water flow from the Manafwa River. However, these walls have shown signs of failure due to erosion, siltation, and poor soil compaction. A 2020 assessment by the Ministry of Agriculture noted that hydraulic instability and Insufficient geotechnical design threaten the scheme’s sustainability.(Wamala et al, 2023).

1.2 Statement of the Problem

The retaining wall at the Doho Flood Irrigation Scheme intake structure is undergoing significant and progressive structural deterioration, which threatens both the stability of the structure and the overall functionality of the irrigation system .The continued weakening of the wall have raised serious concerns about the reliability of water delivery and the safety of communities in the surrounding areas (Bwambale, 2019).

Over time, several maintenance interventions and minor repairs have been carried out to stabilize the wall (Khelalfa, 2025). However, these measures have primarily addressed surface level symptoms rather than the underlying engineering issues. Because these interventions were not based on comprehensive geotechnical and hydraulic assessments, the structural failures have continued to intensify. Visible signs of deterioration, including wall tilting, settlement, and cracking (inclined and vertical), suggest that the structural condition remains critical despite prior mitigation efforts (Ituka, 2022).

The decline in the retaining wall's condition can largely be attributed to design deficiencies that did not adequately consider site specific geotechnical and hydraulic factors at the intake (Wamala et al, 2023). The original design did not fully account for the characteristics of the foundation soil or the magnitude of lateral earth pressures acting on the structure. Consequently, the wall is experiencing a combination of failure mechanisms, including overturning due to excessive lateral forces and reduced bearing capacity caused by erosion and scour of the foundation (Ituka, 2022).

To address this problem, the proposed study will carry out a detailed geotechnical and hydraulic stability assessment of the intake retaining wall (Bwambale, 2019). The investigation will involve determining critical soil parameters such as unit weight, cohesion, internal friction angle, and allowable bearing pressure alongside the wall. The data obtained will be used to calculate the Factors of Safety against overturning, sliding, and bearing capacity failure. The results will inform the development of technically robust, data-driven rehabilitation design recommendations aimed at restoring the wall's long term structural stability (Wamala et al, 2023).

The ongoing deterioration of the wall has already led to reduced efficiency in water conveyance, increased emergency maintenance requirements, and elevated vulnerability to structural collapse. If left unaddressed, these issues could result in operational failures, flooding hazards, and significant disruptions to agricultural activities and community livelihoods. Therefore, a comprehensive assessment and targeted rehabilitation plan are essential to ensure the long-term functionality and safety of the Doho irrigation intake (Wamala et al, 2023).

1.3 Justification of the Study

The Doho Irrigation Scheme has remained operational; however, progressive structural failures such as cracking, tilting, and scouring have increasingly affected the intake retaining wall. These visible signs of distress indicate underlying geotechnical and hydraulic instabilities that may compromise the structural integrity of the intake and threaten reliable water supply to irrigated farmlands. This study was therefore undertaken to characterize the in-situ geotechnical properties of the foundation soils and evaluate the mechanical strength of the retaining wall construction materials (SO1). Understanding these properties provides a reliable basis for assessing soil–structure interaction and identifying potential weaknesses in the supporting materials. The study further developed numerical models to evaluate the geotechnical and hydraulic stability behavior of the retaining wall system under critical loading conditions (SO2). This enabled the identification of dominant failure modes and quantification of the corresponding Factors of Safety. Based on the results obtained, the study developed practical design improvement to enhance the stability and performance of the retaining wall at the intake (SO3). The implementation of these recommendations improves structural reliability, supports continuous irrigation water delivery, and contributes to sustained agricultural productivity, food security, and climate-resilient infrastructure development in Eastern Uganda.

1.4 Objectives of the Study

1.4.1 Main Objective (Purpose of the Study)

The main objective of this study was to assess the geotechnical and hydraulic factors contributing to retaining wall failures at the Doho Irrigation Scheme intake and develop design solutions for enhanced stability

1.4.2 Specific Objectives

The study was guided by the following three specific, progressive objectives.

1. To characterize the in situ geotechnical properties of foundation soils and the mechanical strength of the retaining wall construction materials
2. To develop numerical models for evaluating the geotechnical and hydraulic stability behavior of the retaining wall system
3. To develop design recommendations for enhancing the stability of the retaining wall at the intake.

1.5 Significance of the Study

This research aligns directly with Uganda's national development agenda and global sustainability frameworks, making it a project of strategic significance. The stabilization of the Doho scheme, the largest public rice irrigation scheme in the country, directly supports the Uganda Vision 2040 goal of transforming agriculture from subsistence to profitable, commercial farming, and contributes to the national goal of increasing the irrigated land area by ensuring the longevity of existing critical infrastructure (P, 2013). In the context of global frameworks, the project contributes to several Sustainable Development Goals (SDGs); SDG 2 (Zero Hunger) by safeguarding the water supply necessary for rice production and ensuring food security; SDG 6 (Clean Water and Sanitation), as the diagnostic focus on Insufficient drainageway and the prescriptive redesign (Objective 3) address seepage and water loss, promoting the sustainable management of water resources; and SDG 9 (Industry, Innovation, and Infrastructure), since the core outcome is an optimized design proposal to build resilient infrastructure (Garcia et al., n.d.). Finally, the study supports the United Nations Development Programme (UNDP) mandate on applied water management, inclusive growth, and disaster risk reduction, by enhancing the climate resilience of poor farming communities dependent on the water asset (Jp uganda aids Pdf et el, 2016).

1.6 Research Questions

What are the in-situ geotechnical properties of the foundation soils and the mechanical strength characteristics of the retaining wall construction materials at the Doho Irrigation Scheme intake?

How does the retaining wall system behave under combined geotechnical and hydraulic loading conditions, and what are the resulting Factors of Safety obtained from numerical modeling?

What appropriate structural and drainage design recommendations can be developed to enhance the stability and long-term performance of the retaining wall at the intake?

1.7 Scope of the Study

This study focuses on assessing the geotechnical and hydraulic stability of the retaining wall at the Doho Flood Irrigation Scheme intake structure. The geotechnical investigation includes subsurface exploration through field sampling and laboratory testing to determine key soil parameters such as unit weight, cohesion, angle of internal friction, bearing capacity, and soil classification. In addition, the study evaluates the mechanical condition and strength characteristics of the existing retaining wall construction materials to determine their load-bearing capacity and level of deterioration. The hydraulic assessment considers water-related forces acting on the retaining wall. Numerical simulation tools, including ASDIP Retain and UKDCP software, are used to perform integrated geotechnical and hydraulic stability analyses. These analyses are carried out to determine the Factors of Safety against sliding, overturning, and bearing capacity failure under combined soil and hydraulic loading conditions, and to identify the dominant mode of failure affecting the retaining wall. Based on the combined geotechnical and hydraulic assessment, the study develops engineering design recommendations for improving the stability and performance of the retaining wall. These recommendations include geotechnical measures such as foundation strengthening. The scope of this study is limited specifically to the retaining wall at the intake structure and its associated stability challenges. The study does not include the analysis of other components of the irrigation scheme, such as canals or control structures. In addition, seepage analysis, a cost benefit analysis and the physical implementation or construction of new retaining wall systems are beyond the scope of this study. Instead, the research provides technically sound design recommendations intended to guide future rehabilitation and construction activities.

1.8 Conceptual Framework

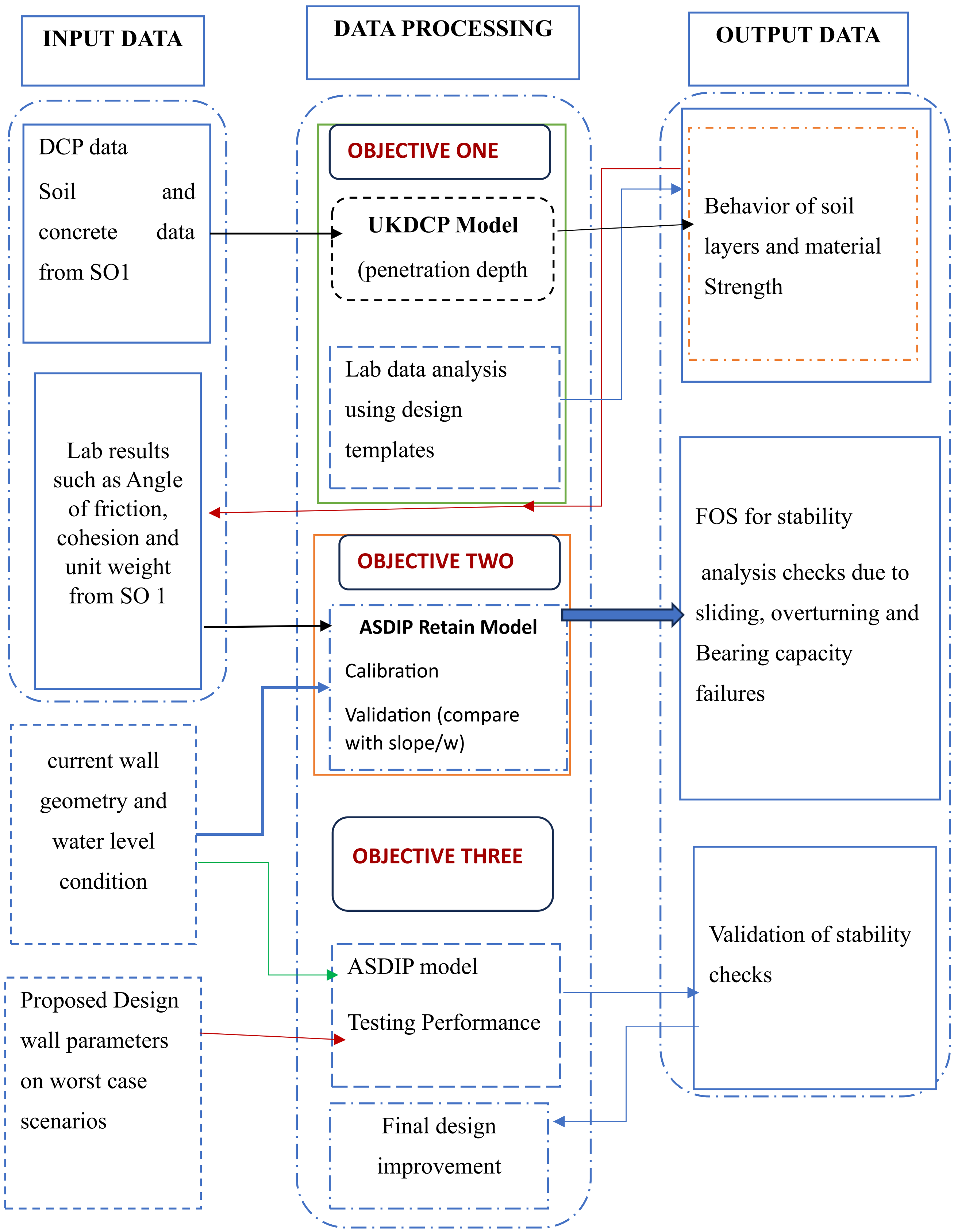

Figure 1:The conceptual flamework of my project proposal.

2 CHAPTER TWO. LITERATURE REVIEW.

2.1 Geotechnical Factors Influencing Retaining Wall Stability

2.1.1 Soil Properties and Backfill Composition

The stability of retaining walls is significantly influenced by the properties of the soil and backfill materials. Studies have shown that poorly compacted backfill or the use of expansive clays can lead to increased hydrostatic pressure behind the wall, contributing to tilting or sliding failures (Dalinghaus Construction, 2024b).

(Makhlouf et al, 2025)conducted a comprehensive evaluation of the failure and rehabilitation strategies of a regulator wing wall in Egypt. They integrated field data, numerical modeling, and material advancements to enhance the stability of hydraulic retaining walls. The study highlighted the importance of understanding the geotechnical and hydrogeological conditions at the site. It emphasized that accurate characterization of soil properties and groundwater conditions is crucial for assessing the stability of retaining walls and for planning effective rehabilitation strategies.

Research gap

While the study provided valuable insights, it lacked detailed in situ testing data and did not employ advanced numerical simulation tools to model the coupled geotechnical hydraulic interactions.

2.1.2 Foundation Design and Compaction

An Insufficient foundation can compromise the wall's stability. Research indicates that a well compacted base with proper anchoring is crucial to prevent sliding and overturning (Stonehsenge Brick Paving and Landscaping, 2024).

2.2 Hydraulic Factors Contributing to Wall Failures

2.2.1 Hydrostatic Pressure

Hydrostatic pressure, resulting from water accumulation behind the wall, is a primary cause of retaining wall failures. Without proper drainage systems, this pressure can cause the wall to bow, lean, or collapse (Dalinghaus Construction, 2024).

(Li et al, 2025) developed a field calibrated numerical model using monitoring data from a water diversion project in Yunnan, China. They employed finite element analysis based on seepage stress coupling theory to analyze the stability of cutoff walls. The study demonstrated the effectiveness of coupled geotechnical hydraulic modeling in assessing the stability of retaining structures under varying hydraulic conditions. It highlighted the importance of integrating seepage and stress analyses to predict potential failure mechanisms accurately.

Research gaps

The study focused on cutoff walls and did not specifically address intake retaining walls. Additionally, it did not explore optimization techniques for enhancing the design and maintenance of the structures.

2.2.2 Drainage Systems

Effective drainage systems, including weep holes and perforated pipes, are essential to alleviate hydrostatic pressure. Insufficient drainage can lead to water pooling behind the wall, increasing the risk of failure (Muthler Landscaping, 2024).

2.3 Case Studies of Retaining Wall Failures

2.3.1 Manistee Riverwalk Collapse

In Michigan, a retaining wall along the Manistee Riverwalk collapsed due to erosion exacerbated by high water levels and storm events. The failure highlighted the importance of considering environmental factors and proper drainage in wall design (Geoengineer.org et al, 2020).

2.3.2 St. Louis Residential Walls

In St. Louis, retaining walls failed due to poor drainage practices, such as the use of clay backfill and lack of proper grading. These cases underscore the necessity of integrating comprehensive drainage solutions in wall construction (RWPS LLC et al, 2024).

(Varga et al, 2024) conducted a comparative analysis of the effects of groundwater, seepage, and hydraulic heave on the optimal design of embedded retaining walls. They used a reliability based and partial factor design approach to optimize the retaining wall design. The study provided insights into optimizing retaining wall designs by considering the effects of groundwater and seepage. It emphasized the need for a reliability-based approach to ensure the long-term stability and performance of retaining structures. The study did not focus on intake retaining walls and lacked detailed maintenance strategies to enhance the long-term performance of the structures.

Critical Synthesis of Literature Review

The reviewed studies collectively emphasize the importance of soil properties, foundation design, and hydraulic factors in retaining wall stability. A recurring theme across (Dalinghaus Construction, 2024), (Stonehenge Brick Paving and Landscaping, 2024), and (RWPS LLC et al, 2024) is the role of backfill compaction and drainage systems in preventing failures. Similarly, (Muthler Landscaping, 2024) and (Geoengineer.org et al, 2020) highlight drainage and environmental conditions as critical contributors to wall collapse. However, while these studies provide descriptive insights, they often lack quantitative geotechnical data and advanced numerical modeling approaches. For instance, (Makhlouf et al, 2025) and (Li et al, 2025) introduced numerical modeling but focused on regulator wing walls and cutoff walls, leaving intake retaining walls underexplored. (Varga et al, 2024) advanced reliability-based design but did not address long-term maintenance strategies.

Identified Research Gap

The literature reveals a gap in integrating site-specific in situ testing data with geotechnical-hydraulic numerical simulations for intake retaining walls. Existing studies either remain descriptive or focus on other wall types, limiting their applicability to irrigation intake structures.

Relevance to Current Study

The present study responds to this gap by combining field-based soil and groundwater characterization with advanced numerical modeling tailored to intake retaining walls. This approach ensures a more accurate assessment of stability and provides practical rehabilitation strategies that directly support irrigation infrastructure resilience.

The literature Review summary in table

Table 1:The summary of literature review.

Author / Year	Focus / Study Area	Key Findings	Identified Gaps	Relevance to current study
Dalinghaus Construction (2024)	Causes of retaining wall failures	Poorly compacted backfill and hydrostatic pressure are major contributors to wall failures	Limited quantitative analysis of soil and water interaction; mostly descriptive	Highlights the importance of proper backfill compaction and hydrostatic pressure management, relevant for irrigation intake walls
Stonehenge Brick Paving & Landscaping (2024)	Retaining wall failures	Reinforcement and drainage integration critical for stability	No site-specific geotechnical data or numerical modeling	Supports design recommendations including drainage systems and soil reinforcement
Muthler Landscaping (2024)	Drainage and wall stability	Ineffective drainage leads to pooling, increased pressure, and wall collapse	Lacks detailed hydraulic modeling or simulation studies	Emphasizes need for integrated drainage design in irrigation intakes
Geoengineer.org (2020)	Case study, Manistee Riverwalk collapse	Erosion and high-water levels caused wall collapse	Limited predictive tools for failure under varying hydraulic loads	Demonstrates impact of environmental conditions, informs risk assessment
RWPS LLC (2024)	St. Louis retaining wall failures	Clay backfills and lack of grading caused failures	No geotechnical measurements or factor of safety analysis	Highlights importance of backfill material selection and foundation grading

3 CHAPTER THREE. METHODOLOGY OF THE STUDY.

This chapter details the systematic engineering procedure used to diagnose the structural failure and formulate the resilient design. The methodology is structured around the three progressive specific objectives.

3.1 To characterize the in situ geotechnical properties of foundation soils and the mechanical strength of the retaining wall construction materials (SO1)

3.1.1 Geography of Doho Irrigation Scheme.

The Doho Irrigation Scheme is located in Himutu Sub-county, Butaleja District, covering approximately 2,500 acres across the parishes of Kangalaba, Wangale, and Kanyenya, including the villages of Masulura and Bwiria. Geographically situated within the River Manafwa floodplain, the scheme utilizes a gravity-fed system to divert water for intensive rice cultivation on fertile alluvial soils. According to (Wamala et al, 2023), while the scheme remains a vital agricultural hub for over 10,000 smallholder farmers, its hydrological performance is frequently challenged by infrastructure deterioration and heavy siltation from the upstream Mt. Elgon catchment. This low-lying terrain experiences a tropical bi-modal rainfall pattern, making the precise management of its canal networks essential for mitigating seasonal flood risks and ensuring consistent water equity (Avery, 2025).

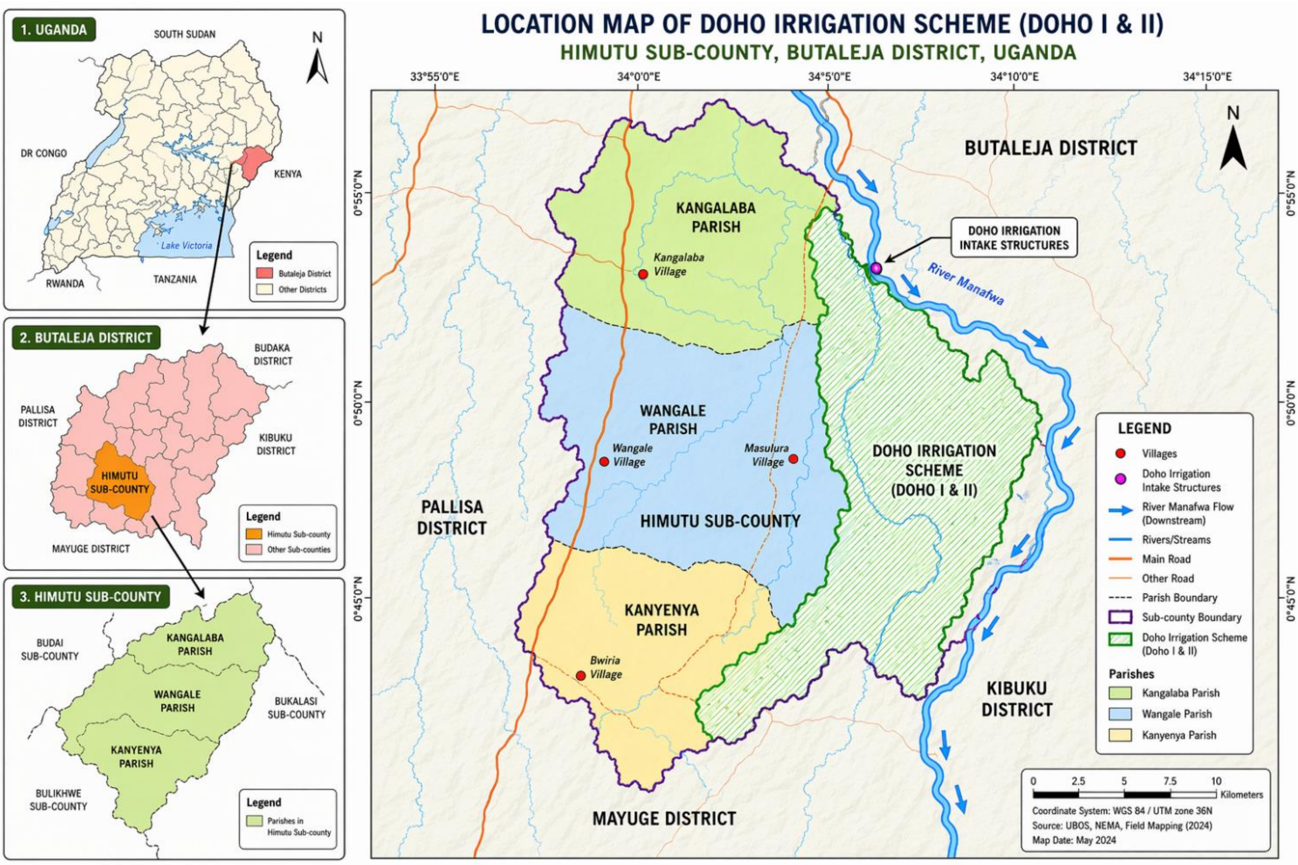

Figure 2:The study area of DOHO Irrigation Scheme in Butaleja district.

3.1.2 Research Instruments and Data Collection

Site Investigation (Soil Sampling). Disturbed soil samples were collected from three test points at depths of 3.0 m, corresponding to the wall foundation levels. Manual excavation of trial pits allowed visual inspection and retrieval of representative samples, with about three taken per depth interval. Laboratory tests focused on shear strength and moisture content, chosen for their relevance to wall stability. Instruments were calibrated with standard references, and results were validated against field observations to ensure accuracy.

Dynamic Cone Penetration (DCP) testing was performed along the failed wall segments to establish the in-situ shear strength profile and identify localized soil softening caused by erosion. The field investigation, including equipment specifications and testing protocols, was conducted in strict adherence to the standardized methodology detailed in ASTM D6951 (ASTM International, 2018). The resulting penetration rates (mm/blow) were utilized to estimate the California Bearing Ratio (CBR) and bearing capacity, following the correlation and data interpretation procedures established by (Done & Samuel, 2004).

3.1.3 Laboratory Testing and Analysis

Standard soil mechanics tests were conducted on collected samples:

Classification Particle size analysis (texture), Atterberg Limits (Plasticity Index) and linear shrinkage to classify the soil type and determine basic index properties (Rutajama, 2000).These tests were done through the following procedures and results;

Determination of Particle size Analysis of soils – wet sieving (Grading).

Particle size distribution (PSD) was conducted as a primary classification test to determine the relative proportions of gravel, sand, silt, and clay within the soil samples, which is essential for predicting the material's engineering behavior. The laboratory testing, encompassing sample preparation, washing, and sieving, was performed in strict accordance with the methodologies and equipment requirements specified in **BS 1377: Part 2: 1990.** Using this standard, soil fractions were categorized based on their retention on specific sieve sizes ranging from clay (passing 0.002 mm) to boulders (retained on 200 mm) to produce a distribution curve used for definitive soil classification and assessment of engineering properties. (British Standards, 2022)

Calculations.

$$\text{Initial Dry Weight} = \left(\frac{\text{Initial weight before washing}}{100 + M.C}\right) \times 100$$

$$\text{Cumulative Retained (\%)} = \left(\frac{\text{Cummulative Retained mass}}{\text{Initial Dry weight}}\right) \times 100$$

$$\text{Percentage passing} = 100 - \text{Cummulative retained percentage}$$

$$\text{Grading Modulus} = 3 - \left(\frac{\%\text{passing } 2.0 + \%\text{passing } 0.425 + \%\text{passing } 0.075}{100}\right) \ldots\ldots\ldots\ldots\ldots\ldots..(1)$$

Plasticity index determination.

Determination of the Plasticity Index (PI) was performed to characterize the consistency and engineering behavior of the cohesive soil samples. The Liquid Limit (LL) and Plastic Limit (PL) were established using the cone penetrometer and the hand-rolling thread techniques, respectively, with specific emphasis on ensuring proper sample maturation for moisture equilibrium. All laboratory procedures were executed in strict adherence to the standardized protocols and equipment specifications defined by the (British Standards, 2022) and the (Ministry of works, 2000) Laboratory Testing Manual. This methodology ensured that the resulting consistency limits provided a reliable basis for soil classification and the assessment of cohesive soil properties.

PI = LL – PL ……………………………………………… (2)

Physical Properties

Determination of Maximum Dry density of soil and Optimum moisture content.

Determination of the Maximum Dry Density (MDD) and Optimum Moisture Content (OMC) was conducted to establish the compaction characteristics necessary for field specifications. The laboratory testing involved heavy compaction using a 4.5 kg rammer and a 152 mm diameter mould, effectively modeling the relationship between compacted dry density and moisture content. All procedures including sample preparation, layer compaction, and the calculation of dry density from bulk density and moisture content were performed in strict adherence to the standardized methodologies defined by the (British Standards, 2022) and the (Ministry of works, 2000) Laboratory Testing Manual. This approach enabled the generation of a compaction curve to accurately identify the MDD and the corresponding OMC required for optimal soil stability and engineering performance.

Calculations

Bulky density (ρ_b) is obtained from;

Bulky density (ρ_b) is obtained from;

$$\rho_b = \left(\frac{\text{mass}}{\text{volume}}\right)$$

and Dry density from;

$$\rho_d = \left(\frac{\rho_b}{100 + M.C}\right) \times 100 \text{..........................} \quad (3)$$

where; ρ_b is the bulky density of the soil.

ρ_d is the dry density of soil.

M.C is the moisture content.

A graph of dry density against moisture content was plotted and the maximum dry density was obtained at a point where the curve just starts to fall and the corresponding moisture content is the optimum moisture content.

Linear Shrinkage determination.

The determination of linear shrinkage was performed to quantify the volumetric reduction of the soil samples during the drying process. This test involved the preparation of a soil specimen at a moisture content approximately equal to its liquid limit, followed by controlled air-drying and subsequent oven-drying in a standardized 140 mm brass mould. The laboratory investigation, including mould preparation, specimen leveling, and the calculation of the percentage shrinkage based on the longitudinal reduction of the soil bar, was conducted in strict adherence to the protocols and equipment specifications defined by the (British Standards, 2022) and the (Ministry of works, 2000) Laboratory Testing Manual. This procedure provided essential data for assessing the expansive potential and shrinkage characteristics of the clayey material.

Calculations.

Linear shrinkage is calculated from;

$$LS = \frac{100(LO - LD)\%}{LO} \quad \ldots\ldots\ldots\ldots\ldots\ldots\ldots\ldots\ldots\ldots\ldots\ldots\ldots..(4)$$

Where; **LD** is the length of the oven-dry specimen (in mm)

LO is the original length of the specimen (in mm)

Determination of the California Bearing Ratio CBR of soil by Three-point method.

The California Bearing Ratio (CBR) was determined using the three-point method to evaluate the subgrade strength and bearing capacity of the soil. The laboratory investigation involved preparing specimens at optimum moisture content and applying varying compactive efforts, utilizing both 4.5 kg and 2.5 kg rammers to establish a correlation between dry density and penetration resistance. Following a four-day soaking period to simulate critical field saturation levels, the specimens were subjected to plunger penetration at a controlled rate to measure resistance at 2.5 mm and 5.0 mm intervals. These procedures, including the calculation of CBR values and the determination of the final strength index at 95% of the maximum dry density, were performed in strict adherence to the standardized protocols in (AASHTO, n.d.)and the (Ministry of works, 2000)0) Laboratory Testing Manual of Tanzania.

Calculations

Equivalent load = 0.2038(ring factor of machine) × DGR

$$\text{Relative compaction} = \left(\frac{\text{dry density}}{\text{MDD}}\right) \times 100 \ldots\ldots\ldots\ldots\ldots\ldots\ldots\ldots\ldots\ldots (5)$$

$$\text{CBR at 2.5 mm} = \left(\frac{\text{equivalent load at 2.5}}{13.2}\right) \times 100 \ldots\ldots\ldots\ldots\ldots\ldots\ldots\ldots\ldots (6)$$

$$\text{CBR at 5.0 mm} = \left(\frac{\text{equivalent load at 5.0}}{19.8}\right) \times 10 \ldots\ldots\ldots\ldots\ldots\ldots\ldots\ldots\ldots\ldots (7)$$

A graph of CBR against Dry Density was plotted and CBR value at 95% of maximum dry density was determined.

Determination of Digital direct shear strength

The determination of direct shear strength parameters, specifically cohesion (c) and the angle of internal friction (ϕ), was conducted using a digital direct shear apparatus integrated with automated data acquisition and processing software. This automated system facilitated high-precision monitoring of the consolidation and shearing phases, allowing for the real-time capture of stress-displacement data and the accurate identification of peak and residual shear stresses. All laboratory operations encompassing specimen preparation, the application of incremental normal stresses, and the generation of the Mohr-Coulomb failure envelope through linear regression were implemented in strict adherence to the standardized protocols defined by the (British Standards, 2022) and the (Ministry of works, 2000) Laboratory Testing Manual of Tanzania. This methodology ensured a highly controlled and efficient workflow for assessing the shear resistance and stability characteristics of the soil.

Determination of compressive strength of collapsed core of concrete using a Rebound harmer.(ASTM International, 2018)

The estimation of the compressive strength of the collapsed concrete cores was conducted through a non-destructive surface hardness assessment using a Schmidt rebound hammer. The investigation involved rigorous surface preparation with an abrasive stone to remove laitance and calibration verification against a steel anvil to ensure instrument accuracy. Rebound readings were recorded by applying the hammer perpendicular to the vertical sides of the secured cores, with a data validation process that included the exclusion of outliers and the averaging of consistent values to derive a representative rebound number (R). These procedures and the subsequent conversion of hardness values into compressive strength estimates were performed in strict adherence to the standardized methodologies defined by (ASTM International, 2018) and the (Ministry of works, 2000) Laboratory Testing Manual of Tanzania.

3.2 To develop numerical models for evaluating the geotechnical and hydraulic stability behavior of the retaining wall system (SO2)

3.2.1 Data Acquisition and Preprocessing

Data were derived from Objective 1, including the **cohesion (c)** and **angle of internal friction (φ)** of the foundation soils. These parameters were used to model the soil structure interaction behavior in ASDIP RETAIN. The soil parameters was obtained from field and laboratory tests in accordance with *ASTM D3080* (direct shear test) (Das & Sobhan, 2018).

3.2.2 Model Calibration

Model calibration was carried out to ensure that the numerical model realistically represents the behavior of the retaining wall under site conditions.

Measured field and laboratory data such as soil shear strength parameters, unit weight, groundwater level, and wall geometry were used as input parameters. An initial model was developed using the mean laboratory values, and simulations were performed iteratively until the computed factors of safety for sliding, overturning, and bearing capacity reflected expected wall performance.

3.2.3 Model Validation

The calibrated model was validated by comparing the stability results obtained from ASDIP RETAIN with those obtained from SLOPE/W using the same soil and geometric input parameters.

The validation focused on the factor of safety against sliding, since sliding represents the most direct measure of overall stability of the retaining wall system under lateral earth pressure. The Factor of Safety (FoS) obtained from ASDIP Retain was therefore compared with the FoS computed using SLOPE/W.

3.2.4 Structural Stability Analysis Using ASDIP Retain

The retaining wall stability was analyzed using **ASDIP RETAIN software**, which performs stability checks in accordance with **ACI 318** and standard geotechnical design procedures (ASDIP Structural Software, 2023).

The modeled geometry includes a tapered concrete stem supported by a footing with specified toe and heel dimensions. The analysis further incorporates the soil cover at the toe and the backfill profile to assess the system's resistance to lateral earth pressures.

3.3 To develop design recommendations for enhancing the stability of the retaining wall at the intake (SO3)

This objective was aimed at translating the results of geotechnical and hydraulic modeling into robust design solutions for the retaining wall at the Doho Irrigation Intake. The design process was based on the **worst-case scenario**, characterized by saturated soils, high groundwater levels, and maximum surcharge loads. The structural performance of the wall was evaluated using **ASDIP Retain software**, and design modifications was proposed to ensure long term stability (Clayton et al, 2014).

Definition of Worst-Case Scenario

To evaluate the robustness of the design, three distinct loading and environmental conditions were simulated:

Baseline Condition (Dry)

A reference model was established to represent the existing wall geometry under normal groundwater levels. This provided a benchmark for stability before adverse hydraulic pressures were introduced.

Combined Adverse Condition

This scenario simulated the simultaneous impact of high groundwater levels and reduced soil shear strength. It was used to determine the geometric limits of the wall required to maintain stability under extreme environmental stress.

Optimized Soil Replacement Condition

A third scenario was modeled to evaluate the impact of improving the backfill and foundation soil properties (increasing the internal friction angle) as an alternative or supplement to massive geometric scaling.

3.3.1 Structural Modeling in ASDIP Retain

The numerical modeling was conducted using ASDIP Retain, adhering to ACI 318 design provisions. The software was used to perform three primary stability checks:

Overturning Stability.

Calculated as the ratio of resisting moments to overturning moments. The model was adjusted to ensure the resisting moment provided by the wall's self-weight and soil overburden sufficiently counteracted the lateral earth and hydrostatic pressures.

$$FoS_{OT} = \frac{M_{resisting}}{M_{overturning}} \geq 1.5 \ldots\ldots\ldots\ldots\ldots\ldots\ldots\ldots\ldots\ldots\ldots\ldots(8)$$

where $M_{resisting}$ is the moment from wall weight and heel soil, and $M_{overturning}$ is due to active earth pressure and surcharge loads (Das & Sobhan, 2018).

Sliding Resistance.

Assessed by comparing the frictional resistance at the base and passive soil resistance against the lateral driving forces. The methodology involved evaluating the effectiveness of both footing extensions and interface friction coefficients.

$$FoS_{SL} = \frac{F_{resisting}}{F_{driving}} = \frac{\mu W + P_{passive}}{P_{active}} \geq 1.5 \ldots\ldots\ldots\ldots\ldots\ldots\ldots\ldots\ldots\ldots(9)$$

where μ is the coefficient of friction between concrete and soil (typically 0.45), W is the wall weight, and P_{active} is the lateral soil pressure from Coulomb's theory (Craig, 2012).

Bearing Capacity.

Determined using the Terzaghi equation to ensure the foundation pressure remained within the safe limits of the soil's ultimate bearing capacity, preventing risk of shear failure or excessive settlement.

$$FS_{bearing} = \frac{q_u}{q_{applied}} \geq 1.0 \ldots\ldots\ldots\ldots\ldots\ldots\ldots\ldots\ldots\ldots\ldots\ldots\ldots\ldots(10)$$

4 CHAPTER FOUR: RESULTS AND DISCUSSIONS

4.1 Results for specific objective one (SO1)

The characterization of the in-situ geotechnical properties and the strength of the retaining wall materials provide a clear diagnostic picture of the structural distress at the Doho Irrigation Scheme intake. The results indicate a fundamental "geotechnical mismatch" between the load-bearing requirements of the structure and the actual capacities of the foundation soil under saturated conditions.

Data analysis report for test sample point one.

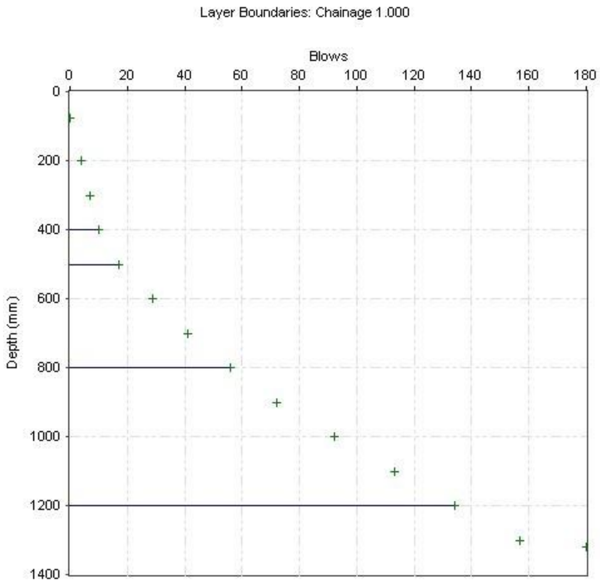

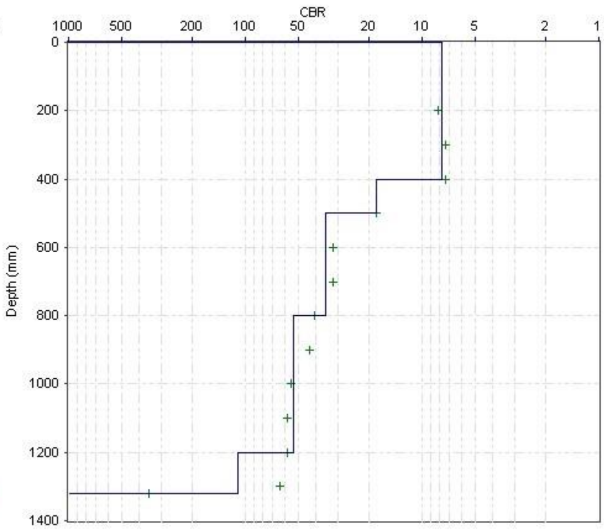

Layer Boundaries Chart

CBR Chart

Figure 3: The layer boundaries chart and CBR chart for the soils

Table 2:Layer properties of first layer penetration by DCP

Layer Properties

No.	Penetration Rate (mm/blow)	CBR (%)	Thickness (mm)	Depth to layer bottom (mm)
1	32.20	8	400	400
2	14.29	18	100	500
3	7.69	35	300	800
4	5.13	54	400	1200
5	2.61	110	120	1320

CBR Relationship:

TRL equation: $\log_{10}(CBR) = 2.48 - 1.057 \times \log_{10}(Strength)$

Report result analysis for test sample point two.

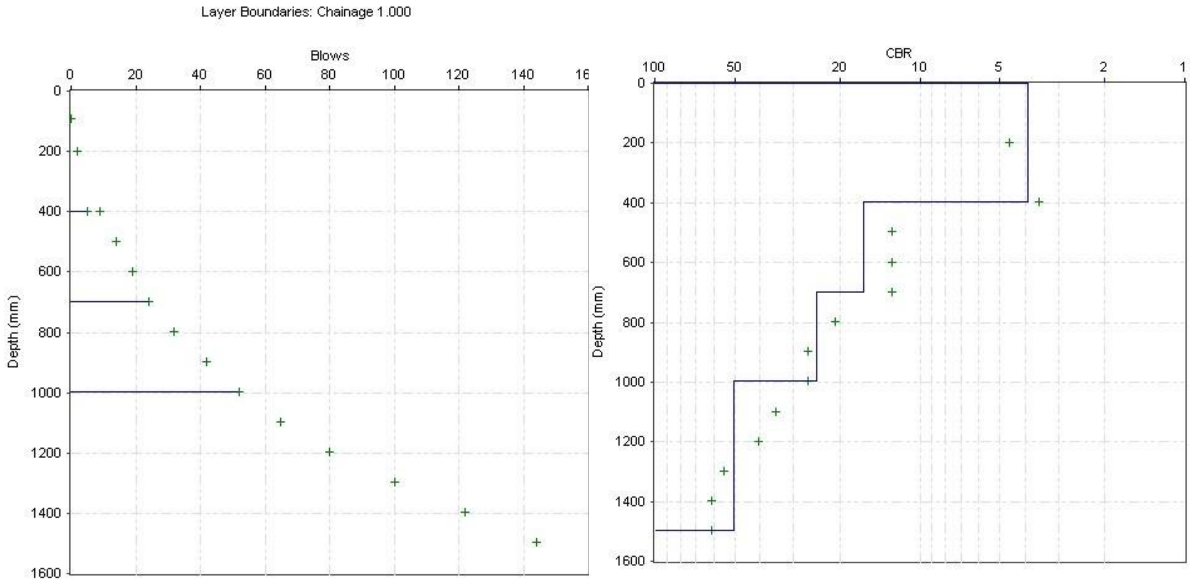

Layer Boundaries Chart CBR Chart

Figure 4: The layer boundaries chart and CBR Chart of soils for second penetration

Table 3:The layer properties of second layer penetration by DCP

Layer Properties

No.	Penetration Rate (mm/blow)	CBR (%)	Thickness (mm)	Depth to layer bottom (mm)
1	61.00	4	398	398
2	15.79	16	300	698
3	10.71	25	300	998
4	5.43	50	500	1498

CBR Relationship:

TRL equation: $\log_{10}(CBR) = 2.48 - 1.057 \times \log_{10}(Strength)$

Report analysis for test sample point three

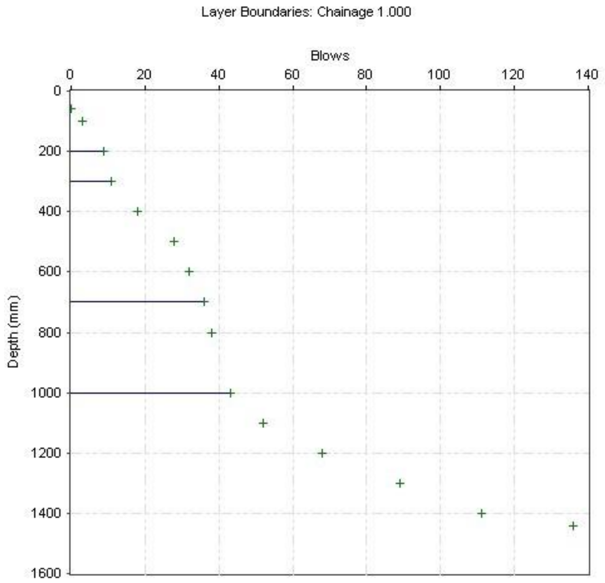

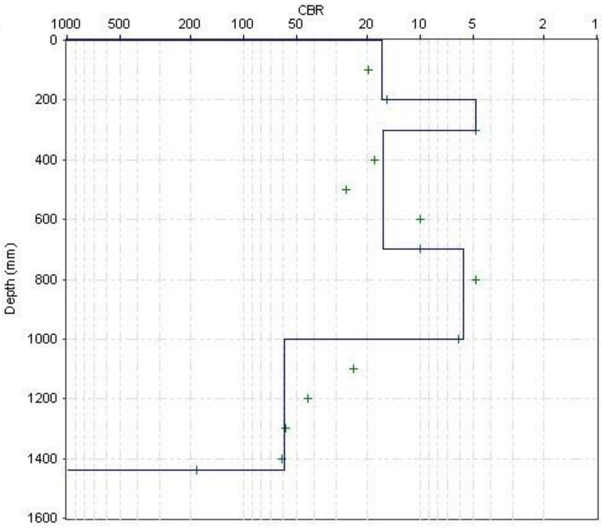

Layer Boundaries Chart CBR Chart

Figure 5: The layer boundaries Chart and CBR Chart of soils for third penetration point

Table 4:The layer properties of third layer penetration by DCP

Layer Properties

No.	Penetration Rate (mm/blow)	CBR (%)	Thickness (mm)	Depth to layer bottom (mm)
1	15.56	17	200	200
2	50.00	5	100	300
3	16.00	16	400	700
4	42.86	6	300	1000
5	4.73	58	440	1440

CBR Relationship:

TRL equation: $\log_{10}(CBR) = 2.48 - 1.057 \times \log_{10}(\text{Strength})$

From table 1, 2 and 3 of penetration results, The DCP analysis at the DOHO irrigation intake reveals a critical deficiency in the subgrade strength of the upper soil horizons, particularly at Test Points 1 and 2, where CBR values as low as 4% to 8% were recorded within the first 400mm. These findings indicate that the soil in its "Wet" state lacks the necessary shear strength to support the heavy vertical and lateral loads imposed by a retaining structure. According to (Das and Sobhan, 2013), soils with a CBR value below 10% are generally classified as poor subgrade, often requiring stabilization or deep foundation strategies to prevent bearing capacity failure. The erratic strength profile observed at TP3, characterized by "soft pockets" of 5% CBR at deeper intervals, suggests non-homogeneous soil conditions likely caused by localized saturation or organic inclusions. In the context of the DOHO intake, these results suggest that if the retaining walls were founded at shallow depths, they were resting on a highly compressible and weak stratum, making them susceptible to the overturning and settling observed in the field.

Comparative Analysis and Scholarly Context

These results align closely with the research of (Sivakumar et al, 2015), who demonstrated that in irrigation and hydraulic environments, the constant presence of water leads to increased pore water pressure and a significant reduction in the effective stress of the soil. This phenomenon explains the extremely low CBR values found in the "Wet" samples at DOHO, as saturated conditions effectively lubricate soil particles and reduce internal friction. Furthermore, the reliance on the TRL equation for DCP interpretation in this study is supported by Kleyn (1975), who established that DCP penetration rates are a reliable proxy for assessing in-situ shear strength in tropical soils. While previous studies by (Jones and Smith, 2020) on similar irrigation schemes suggested that wall failures are often due to poor masonry quality, the data from this study indicates that at the DOHO site, the primary driver of failure is more likely the geotechnical instability of the foundation soil rather than the structural material itself. Consequently, the findings corroborate the theory that the interaction between high moisture levels and low-strength silty/clayey layers at the intake site is the fundamental cause of the structural distress.

From shear strength test, the geotechnical analysis reveals that the DOHO intake soil possesses a critically low allowable bearing capacity recorded as low as 35 kPa at 1.0m depth, alongside poor DCP results (CBR 4–8%). These values indicate a highly compressible subgrade that is insufficient for supporting heavy retaining structures. According to (Das and Sobhan, 2013), such low bearing parameters often trigger "Local Shear Failure," a mechanism where the soil fails to resist structural loads, leading to the tilting and settlement observed at the site. As noted by (Varghese, 2021), foundations in these conditions are prone to instability because the load exceeds the soil's internal shear resistance, confirming that the wall foundations were likely under-designed for the actual ground conditions.

The failure is further aggravated by high moisture levels at the irrigation intake, which reduced the soil's friction angle to a mere11∘ at Test Point 1. Modern research by (Zhang et al, 2020) confirms that in hydraulic environments, increased saturation drastically lowers effective stress and shear strength, explaining the "soft pockets" and erratic strength profiles found in the DCP data. This saturation-induced softening is a primary driver of infrastructure distress in irrigation schemes (Sadek et al, 2023). Consequently, the results prove that the wall failures at DOHO are caused by a geotechnical mismatch. the foundation soil lacks the necessary shear strength to remain stable under the saturated, high-moisture conditions inherent to an active irrigation intake. The table of results of shear is as shown below.

Table 5:Compressive strength of the core

Test number	Compressive strength values (Mpa)
1	22.0
2	23.0
3	21.6
Average	**22.2**

Table 6:Summary of data from specific objective one (SO1)

Soil layers	1	2	3
Description of materials	Blackish grey	Reddish brown	Darkish grey
MDD (g/cm3)	1.50	1.68	1.79
OMC (%)	12.5	11.9	10.0
GM	0.37	0.79	0.86
PI (%)	30.1	28.8	24.8
Soaked CBR at 95%	21.0	24	30
Cohesion force (Kpa)	14	9	8
Internal angle of friction (degrees)	11	26	32
Shear strength (Kpa)	29.42	49.03	34.32
Linear shrinkage (%)	15.0	13.6	12.1
Compressive strength of failed Concrete core (Mpa)		22.2	

The results summarized in Table 6 characterize the foundation environment at the DOHO irrigation intake as a highly challenging geotechnical setting. The following discussion analyzes these parameters in the context of structural resilience and failure mechanisms.

Analysis of Plasticity and Volumetric Stability

The Plasticity Index (PI) across the layers (24.8% to 30.1%) and the Linear Shrinkage (LS) values (12.1% to 15.0%) indicate that the foundation consists of highly plastic and expansive soils. According to (Abbas et al, 2020), soils with a PI exceeding 20% are classified as having high swelling potential, which can exert significant upward swelling pressure on foundations during wet seasons.

The high LS values are particularly problematic. (Bhattacharjee and Gunda, 2021) suggest that linear shrinkage above 10% indicates a soil prone to severe desiccation cracking. In the context of the DOHO intake, the "Wet" and "Moderate" field moisture conditions recorded suggest that these soils undergo significant volume changes during irrigation cycles. This cyclical shrinking and swelling likely created voids beneath the retaining wall, leading to differential settlement and the eventual collapse of the structure.

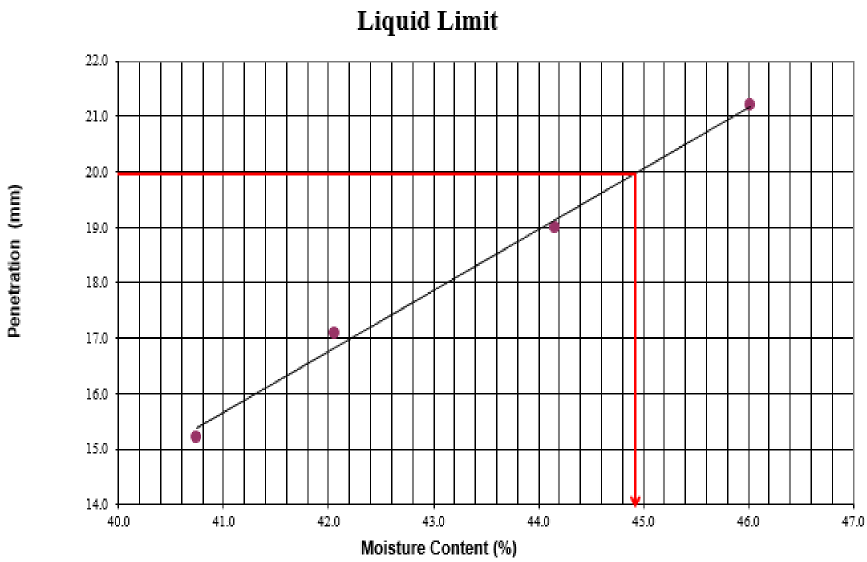

As received / washed on 425 mic sieve / oven dried at 110°C

RESULTS	
Liquid limit (%)	44.9
Plastic limit (%)	14.7
Plasticity index	30.1

Reported plasticity index(PI) =	**30.1**

Figure 6:The Plasticity Index (PI) and Linear shrinkage (LS)

Shear Strength and Stability Implications

Layer 1 (Blackish grey) presents a critical weakness with an internal angle of friction (ϕ) of only 11° and a cohesion of 14 kPa.

Comparison, (Das and Sobhan, 2021) state that for stable retaining wall foundations, the friction angle of the base soil should ideally exceed 25° to provide adequate resistance against sliding.

Analysis: The recorded 11° is significantly below the safety threshold. This suggests that Layer 1 acted as a "slip plane." When the soil became saturated (as noted in the field DCP report), the effective stress decreased, further reducing the shear strength. This matches the findings of (Ng et al, 2019), who demonstrated that rainfall-induced saturation in high-plasticity clays drastically reduces the factor of safety for gravity walls, often leading to sudden lateral displacement.

Compaction and Subgrade Strength (CBR)

The soaked CBR values range from 21% to 30%. While these values suggest a "fair to good" subgrade under laboratory-controlled compaction, they must be viewed with caution.

Comparison, (Tiza et al, 2021) noted that in irrigation and hydraulic zones, laboratory CBR often overestimates in situ strength because it does not account for the continuous seepage and "pumping" effect of fluctuating water tables.

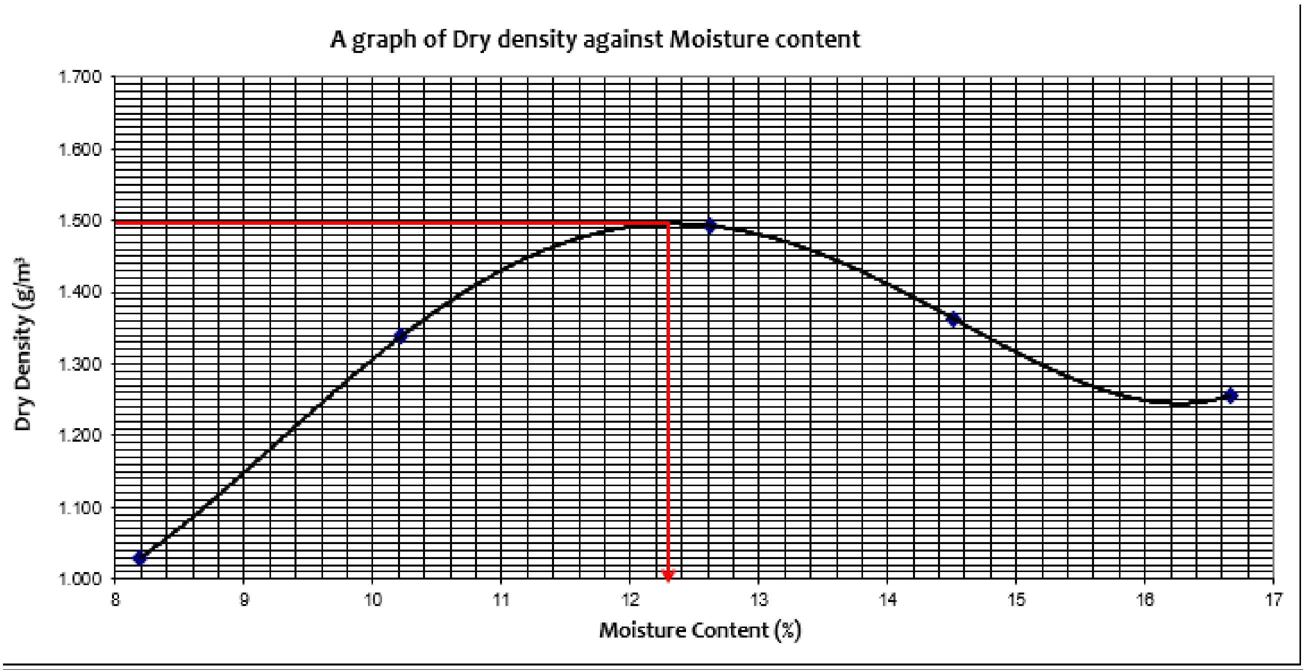

MDD:	1.500	(g/cm3)		OMC:	12.5	(%)

Figure 7:Maximum Dry Density and Optimum moisture content of the first layer of soil.

Analysis, The MDD of 1.50 g/cm³ in Layer 1 is relatively low, indicating a loose soil fabric that is susceptible to moisture ingress. The discrepancy between the laboratory CBR and the "softening" observed during the DCP field test indicates that the wall's foundation was compromised by localized saturation that laboratory tests (conducted on remolded samples) could not fully simulate.

Concrete Material Integrity

The rebound hammer test yielded an average compressive strength of 22.2 MPa.

Comparison: For hydraulic structures exposed to aggressive moisture environments and potential scouring, ACI 318-19 (ACI 318-19, 2019) and (BS EN, 2023) recommend a minimum durability class of C25/30 (approx. 30 MPa).

Analysis, the 22.2 MPa result indicates that the concrete was likely a Class 20 mix. While sufficient for minor load-bearing, it lacks the density and strength required to resist the lateral pressures exerted by the heavy, plastic clay backfill. The failure confirms that the wall's material strength was marginal for the environmental demands of an irrigation intake.

4.2 Results for specific objective two (SO2)

4.2.1 Model Calibration and Validation Results

The results of the calibration and validation processes demonstrate the reliability of the numerical models used to assess the retaining wall's stability.

Through the iterative calibration process described in Section 3.2.2, the initial model parameters were refined to align with site specific laboratory data. The calibration ensured that the baseline model produced factors of safety for bearing capacity and overturning that were consistent with the theoretical expectations for the wall's geometry and the observed soil conditions.

As specified in the methodology, the model's accuracy was validated by comparing the Factor of Safety (FoS) against sliding generated by ASDIP RETAIN and SLOPE/W. The sliding stability was selected as the primary validation metric because it is the most sensitive to variations in lateral earth pressure and interface friction.

The comparative results are summarized in Table 7 below.

Table 7:The comparison of sliding factor of safety for validation of the ASDIP Retain.

Model	**Factor of safety (sliding)**
Slope/w	0.60
ASDIP Retain	0.64

Discussion of Model Validation

The validation of the numerical model showed a percentage difference of 6.67% between SLOPE/W (0.60) and ASDIP Retain (0.64). In the context of modern computational geotechnics, this variance is highly acceptable. According to (Sazzad and Islam, 2021), comparative studies between different limit equilibrium and structural analysis software typically yield variances between 5% and 12% due to differences in how nodal pressures and soil structure interfaces are discretized. This validation confirms that ASDIP Retain is a reliable tool for simulating the lateral earth pressures specific to the Doho Irrigation site.

4.2.2 The ASDIP Retain model results

The Gravity wall geometry consisted of a concrete stem with a height of 2.60 m, a top thickness of 0.30 m, and a bottom thickness of 0.90 m. The footing thickness was 0.30 m, with a toe length of 0.30 m and a heel length of 0.90 m. Additionally, the soil cover at the toe was 0.30 m, and the backfill height was 2.60 m with a backfill slope angle of 0.0 degrees.

Regarding applied loads, the dead and live surcharge were recorded at D = 0.0 and L = 0.0 KPa, respectively, while the stem vertical and horizontal loads were both recorded as D = 0.0 and L = 0.0 KN/m. The eccentricity was noted as ev = 15.2 cm and eh = 15.2 cm. Finally, the wind load was specified as 0.0 KPa at a height of 1.52 m.

Backfill Properties

Wall taper: α = aTan (taper / H) = aTan ((0.9 - 0.3) / 100 / 2.60) = 0.115 rad

Backfill slope: β = slope * π / 180 = 0.0 * π / 180 = 0.000 rad

Internal friction: φ = Int. friction * π / 180 = 11.0 * π / 180 = 0.192 rad

Wall-soil friction: δ = φ / 2 = 0.192 / 2 = 0.096 rad

Seismic angle: θ = aTan (kh / (1 - kv)) = aTan (0.00 / (1 - 0.00)) = 0.000 rad

Footing length ftg = toe + stem + heel = 0.30 + 0.90 / 100 + 0.90 = 2.10 m

Height for Stability Hs = wedge + backfill + footing = 0.00 + 2.60 + 0.3 / 100 = 2.90 m

Earth pressure theory = Coulomb Active

Moist density = 17 KN/m³

Saturated density = 18 KN/m³

Active coefficient $k_a = \dfrac{\cos^2(\phi+\alpha)}{\cos^2\alpha \cdot \cos(\delta+\alpha) \cdot \left[1+\left(\dfrac{\sin(\phi+\delta)\cdot\sin(\phi-\beta)}{\cos(\delta+\alpha)\cdot\cos(\beta-\alpha)}\right)^{1/2}\right]^2} = 0.67$

Active pressure $p_a = k_a \cdot \gamma = 0.67 \cdot 16.5 = 11.1$ KPa/m of height

For stability analysis (non-seismic)

Active force $P_a = k_a \cdot \gamma \cdot H_s^2/2 = 0.67 \cdot 16.5 \cdot 2.90^2/2 = 46.8$ KN/m

$$P_{ah} = P_a \cdot \cos(\delta + \alpha) = 46.8 \cdot \cos(0.096 + 0.115) = 45.7 \text{ KN/m}$$

$$P_{av} = P_a \cdot \sin(\delta + \alpha) = 46.8 \cdot \sin(0.096 + 0.115) = 9.8 \text{ KN/m}$$

Water force $P_w = (k_a \cdot (\gamma_s - \gamma_{ww} + \gamma_w) \cdot (\text{water table})^2/2$

$$P_w = (0.67 \cdot (18.3 - 9.8 - 16.5) + 9.8) \cdot 2.30^2/2 = 11.7 \text{ KN/m}$$

Passive coefficient $k_p = \dfrac{\cos^2(\phi+\alpha)}{\cos^2\alpha \cdot \cos(\delta-\alpha) \cdot \left[1 - \left(\frac{\sin(\phi+\delta)\cdot\sin(\phi+\beta)}{\cos(\delta-\alpha)\cdot\cos(\beta-\alpha)}\right)^{1/2}\right]^2} = 1.57$

For stem design (non-seismic)

Active force $Pae = kae \cdot \gamma \cdot H^2/2 = 0.67 \cdot 16.5 \cdot 2.60^2/2 = 37.6$ KN/m

$$Pah = Pa \cdot \cos(\delta + \alpha) = 37.6 \cdot \cos(0.096 + 0.115) = 36.8 \text{ KN/m}$$

$$Pav = Pa \cdot \sin(\beta) = 37.6 \cdot \sin(0.000) = 0.0 \text{ KN/m}$$

Water force $Pw = (ka \cdot (\gamma_s - \gamma_w - \gamma) + \gamma_w) \cdot (Water\ table - Ftg)^2/2$

$$Pw = (0.67 \cdot (18.3 - 9.8 - 16.5) + 9.8) \cdot (2.30 - 0.3/100)^2/2 = 8.8 \text{ KN/m}$$

Hor. seismic coeff. $kh = 0.00$, Ver. seismic coeff. $kv = 0.00$

Active seismic coef. $kae =$

$$\frac{\cos(\phi-\alpha-\theta)}{\cos\theta \cdot \cos^2\alpha \cdot \cos(\delta+\alpha+\theta) \cdot \left[1 + \left(\frac{\sin(\phi+\delta)+\sin(\phi-\beta-\theta)}{\cos(\delta+\alpha+\theta)\cdot\cos(\beta-\alpha)}\right)^{1/2}\right]^2} = 0.67$$

For stability analysis (seismic)

Seismic force $Pae = kae \cdot \gamma \cdot H_s^2/2 \cdot (1 - kv) = 0.67 \cdot 16.5 \cdot 2.90^2/2 \cdot (1 - 0.0) = 46.8$ KN/m

$$Paeh = Pae \cdot \cos(\delta + \alpha) = 46.8 \cdot \cos(0.096 + 0.115) = 45.7 \text{ KN/m}$$

$$Paev = Pae \cdot \sin(\delta + \alpha) = 46.8 \cdot \sin(0.096 + 0.115) = 9.8 \text{ KN/m}$$

Water force $Pwe = kh \cdot (\gamma_s - \gamma) \cdot (water)^2/2$

$$Pwe = 0.00 \cdot (18.3 - 16.5) \cdot (2.30)^2/2 = 0.0 \text{ KN/m}$$

For stem design (seismic)

Seismic force $Pae = kae \cdot \gamma \cdot H^2/2 = 0.67 \cdot 16.5 \cdot 2.60^2/2 = 37.6$ KN/m

$$Paeh = Pae \cdot \cos(\delta + \alpha) = 37.6 \cdot \cos(0.096 + 0.115) = 36.8 \text{ KN/m}$$

$$Paev = Pae \cdot \sin(\delta + \alpha) = 37.6 \cdot \sin(0.096 + 0.115) = 7.9 \text{ KN/m}$$

Water force $Pwe = kh \cdot (\gamma_s - \gamma) \cdot (water\ table - ftg)^2/2$

$$Pwe = 0.00 \cdot (18.3 - 16.5) \cdot (2.30 - 0.3/100)^2/2 = 0.0 \text{ KN/m}$$

OVERTURNING CALCULATIONS (Comb. D + H + 0.6W)

Overturning Forces

Backfill = Lat factor · Pah = 1.00 · 45.7 = 45.7 KN/m Arm = Hs / 3 = 2.90 / 3 = 0.97 m

Moment = 45.7 · 0.97 = 44.2 KN-m/m

Water table = Lat factor · Pw = 1.00 · 11.7 = 11.7 KN/m

Arm = Water table / 3 = 2.30 / 3 = 0.77 m Moment = 11.7 · 0.77 = 8.9 KN-m/m

Surcharge = Factor · ka · Surcharge · Hs · Cos (δ + α) = 1.00 · 0.67 · 0.0 · 2.90 · 0.98 = 0.0 KN/m Arm = Hs / 2 = 2.90 / 2 = 1.45 m Moment = 0.0 · 1.45 = 0.0 KN-m/m

Concentrated Horizontal = Factor · Ph = 1.00 · 0.00 + 0.00 · 0.00 = 0.0 KN/m

Arm = Stem + Flg – Ecc / 100 = 2.60 + 0.30 – 15.2 / 100 = 2.75 m

Moment = 0.0 · 2.75 = 0.0 KN-m/m

Wind load = WL factor · Pressure · Wind height = 0.60 · 0.0 · 1.52 = 0.0 KN/m

Arm = Flg + Stem – Wind height / 2 = 0.30 + 2.60 – 1.52 / 2 = 2.14 m

Moment = 0.0 · 2.14 = 0.0 KN-m/m

Backfill seismic = EQ factor · (Paeh – Pah Coulomb) = 0.00 · (45.7 – 45.7) = 0.0 KN/m

Arm = 0.6 · Hs = 0.6 · 2.90 = 1.74 m Moment = 0.0 · 1.74 = 0.0 KN-m/m

Water seismic = EQ factor · Pwe = 0.00 · 0.0 = 0.0 KN/m

Arm = Water table / 3 = 2.30 / 3 = 0.77 m Moment = 0.0 · 0.77 = 0.0 KN-m/m

Wall self-weight seismic effect not considered in calculations

Wall seismic = 0.0 KN Moment = 0.0 KN-m/m

Passive force = 0.0 KN/m (**Ignore passive pressure in overturning**)

Arm = 0.20 m Moment = 0.0 · 0.20 = 0.0 KN-m/m

Overturning force $Rh = 45.7 + 11.7 + 0.0 + 0.0 + 0.0 + 0.0 + 0.0 + 0.0 + 0.0 + 0.0 - 0.0 =$ 57.4KN/m

Overturning moment $OTM = 44.2 + 8.9 + 0.0 + 0.0 + 0.0 + 0.0 + 0.0 + 0.0 + 0.0 + 0.0 - 0.0 =$ 53.2KN-m/m

Arm of horizontal resultant $= OTM/Rh = 53.2/57.4 = 0.93$m

Resisting Forces

Stem top $W_{Stem} = DL\ factor \cdot Thickness \cdot Height \cdot \gamma_c = 4.00 \cdot 0.30 \cdot 2.60 \cdot 24.00 = 18.7$KN/m
Arm = Toe + Taper + Thick / 2 = 0.30 + 0.30 + 0.30 / 2 = 0.75 m

Moment = 18.7 · 0.75 = 14.0 KN-m/m

Stem taper toe $= DL\ factor \cdot \Delta Thick \cdot Height/2 \cdot \gamma_c = 1.00 \cdot 0.30 \cdot 2.60/2 \cdot 24.00 = 9.4$KN/m Arm = Toe + Thick · 2 / 3 = 0.30 + 0.30 · 2 / 3 = 0.50 m

Moment = 9.4 · 0.50 = 4.7 KN-m/m

Stem taper heel $= DL\ factor \cdot \Delta Thick \cdot Height/2 \cdot \gamma_c = 1.00 \cdot 0.30 \cdot 2.60/2 \cdot 24.00 = 9.4$KN/m

Arm = Toe + Taper + Top + Thick / 3 = 0.30 + 0.30 + 0.30 + 0.30 / 3 = 1.00 m Moment = 9.4 · 1.00 = 9.4 KN-m/m

Footing weight $W_{FtG} = DL\ factor \cdot Length \cdot Thickness \cdot \gamma_c = 1.00 \cdot 2.10 \cdot 0.30 \cdot 24.00 =$ 15.1KN/m Arm = Length / 2 = 2.10 / 2 = 1.05 m Moment = 15.1 · 1.05 = 15.9 KN-m/m

Soil cover $= DL\ factor \cdot Toe \cdot Soil\ cover \cdot \gamma = 1.00 \cdot 0.30 \cdot 0.30 \cdot 16.5 = 1.5$KN/m Arm = Toe / 2 = 0.30 / 2 = 0.15 m Moment = 1.5 · 0.15 = 0.2 KN-m/m

Stem wedge $= DL\ factor \cdot \Delta Thick \cdot Height/2 \cdot \gamma = 1.00 \cdot 0.30 \cdot 2.60/2 \cdot 16.5 = 6.4$KN/m Arm = Toe + Thick – \Delta Thick · 2 / 3 = 0.30 + 0.90 – 0.30 · 2 / 3 = 1.10 m

Moment = 6.4 · 1.10 = 7.1 KN-m/m

Backfill weight $= DL\ factor \cdot Heel \cdot Height \cdot \gamma = 1.00 \cdot 0.90 \cdot 2.60 \cdot 16.5 = 38.6$ KN/m

Arm = Ftg – Heel / 2 = 2.10 – 0.90 / 2 = 1.65 m Moment = 38.6 · 1.65 = 63.7 KN-m/m

Backfill slope $= DL\ factor \cdot (Heel + \Delta Thick) \cdot Wedge/2 \cdot \gamma = 1.00 \cdot (0.9 + 0.30) \cdot 0.00/2 \cdot 16.5 = 0.0$ KN/mArm = Ftg – Heel – Δ Thick / 3 = 2.10 – 0.90 – 0.30 / 3 = 1.10 m

Moment = 0.0 · 1.10 = 0.0 KN-m/m

Water $= Factor \cdot Heel \cdot (Water–Ftg) \cdot (\gamma_s–\gamma) = 1.00 \cdot 0.90 \cdot (2.30–0.30) \cdot (18.3–16.5) =$ 3.2 KN/mArm = Ftg – Heel / 2 = 2.10 – 0.90 / 2 = 1.65 m Moment = 3.2 · 1.65 = 5.3 KN-m/m

Seismic backfill $= EQ\ factor \cdot (P_{aev}–P_{av}) = 0.00 \cdot (9.8–9.8) = 0.0$ KN/m

Arm = Footing length = 2.10 m Moment = 0.0 · 2.10 = 0.0 KN-m/m

Backfill $P_{av} = Lat\ factor \cdot P_{av} = 1.00 \cdot 9.8 = 9.8$ KN/m

Arm = Footing length = 2.10 m Moment = 9.8 · 2.10 = 20.6 KN-m/m

Concentrated $= Factor \cdot Vert.\ load = 1.00 \cdot 0.0 + 0.00 \cdot 0.0 = 0.0$ KN/m

Arm = Toe + Taper + Stem / 2 – Ecc / 100 = 0.30 + 0.30 · 0.30 / 2 – 15.2 / 100 = 0.60 m Moment = 0.0 · 0.60 = 0.0 KN-m/m

Surcharge $= Srch\ factor \cdot (Heel + \Delta Thick) \cdot Surcharge = (1.00 \cdot 0.0 + 0.00 \cdot 0.0) \cdot (0.90 + 0.30) = 0.0$ KN/mArm = Ftg – (Heel + ΔThick) / 2 = 2.10 – (0.90 + 0.30) / 2 = 1.50 m Moment = 0.0 · 1.50 = 0.0 KN-m/m

Buoyancy $= DL\ factor \cdot \gamma_w \cdot Water\ table \cdot Ftg = 1.00 \cdot 9.8 \cdot 2.30 \cdot 2.10 = -47.4$ KN/m

Arm = Footing / 2 = 2.10 / 2 = 1.05 m Moment = -47.4 · 1.05 = -49.8 KN-m/m

Vertical resultant $R_v \Sigma$ Vertical forces = 64.7 KN/m

Resisting moment $RM \Sigma$ Moments = 91.1 KN-m/m

Arm of vertical resultant $= RM/R_v = 91.1/64.7 = 1.41$ m

Overturning Safety Factor $= RM/OTM = 91.1/53.2 = 1.71 > 1.50$ OK

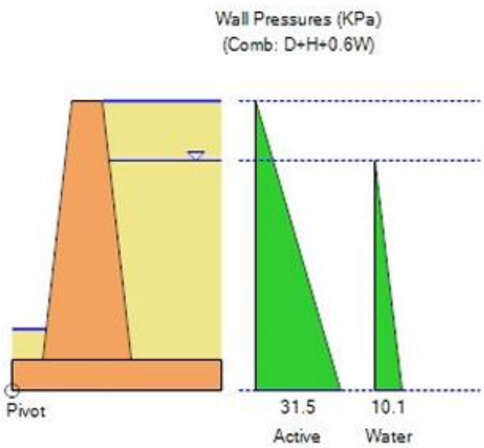

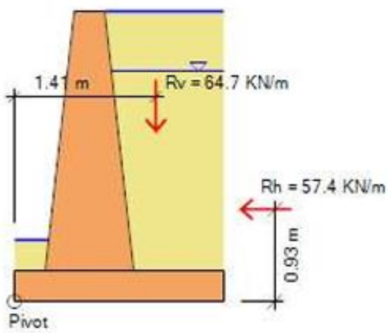

SOIL BEARING PRESSURES (Comb. D + H + 0.6W)

Eccentricity $= (Ftg/2) - (RM - OTM)/R_v = 2.10/2 - (91.1 - 53.2)/64.7 = 0.46$ m

Bearing length $= \text{Min}(Ftg, 3 \cdot (Ftg/2 - Ecc)) = \text{Min}(2.10, 3 \cdot (2.10/2 - 0.46)) = 1.76$ m

Toe bearing $= R_v/(0.75 \cdot Ftg - 1.5 \cdot Ecc) = 64.7/(0.75 \cdot 2.10 - 1.5 \cdot 0.46) = 73.6$ KN/m^2 $>$ 0.0 KN/m^2 NG

Heel bearing $= 0.0$ KN/m^2

SLIDING CALCULATIONS (Comb. D + H + 0.6W)

Sliding force $Rh = 45.7 + 11.7 + 0.0 + 0.0 + 0.0 + 0.0 + 0.0 + 0.0 = 57.4$ KN/m

Passive coefficient k_p (Coulomb) $= 1.57$

Passive depth D_p = Soil cover + Ftg − Neglect depth $= 0.30 + 0.30 - 0.00 = 0.60$ m

Passive pressure top $= k_p \cdot \gamma' \cdot$ (Neglect depth) + Water $= 1.57 \cdot 16.5 \cdot 0.00 + 0.00 = 0.00$ KN/m^2

Passive pressure bottom $= k_p \cdot \gamma' \cdot (D_p +$ Neglect depth) + Water $= 1.57 \cdot 16.5 \cdot (0.60 + 0.00) + (-1.65) = 13.87$ KN/m^2

Passive force = (Pressure top + Pressure bottom)$/2 \cdot D_p = (0.00 + 13.87)/2 \cdot 0.60 = 4.2$ KN/m

Friction force $= \text{Max}(0, R_v \cdot$ Friction coeff.) $= \text{Max}(0, 64.7 \cdot 0.50) = 32.4$ KN/m

Sliding S.F. = (Passive + Friction)$/Rh = (4.2 + 32.4)/57.4 = 0.64 < 1.50 NG$

STEM DESIGN (Comb. 1.2D + 1.6L + 1.6H)

Backfill = Lat factor $\cdot P_{ah} = 1.6 \cdot 36.8 = 58.8$ KN/mArm = Hb / 3 = 2.60 / 3 = 0.87 m Moment = 58.8 · 0.87 = 51.0 KN-m/m

Water table = Factor $\cdot P_w = 1.6 \cdot 8.8 = 14.1$ KN/mArm = (Water table – Ftg) / 3 = (2.30 – 0.3 / 100) / 3 = 0.77 m Moment = 14.1 · 0.77 = 9.4 KN-m/m

Surcharge = Factor $\cdot k_a \cdot$ Surcharge $\cdot H_s \cdot \cos(\delta + \alpha) = 1.6 \cdot 0.67 \cdot 0.0 \cdot 2.60 \cdot 0.98 =$ 0.0 KN/mArm = Hb / 2 = 2.60 / 2 = 1.30 m

Moment = 0.0 · 1.30 = 0.0 KN-m/m

Vert. Concentrated = Factor · Shear $= 1.2 \cdot 0.0 = 0.0$ KN/m

Moment = 1.2 · 0.0 · 1.6 · 0.0 = 0.0 KN-m/m

Hor. Concentrated = Factor · Load $= 1.2 \cdot 0.0 = 0.0$ KN/m

Moment = 0.0 · 1.60 · 0.0 = 0.0 KN-m/m

Arm = Stem – Ecc = 2.60 – 15.2 / 100 = 2.45 m Moment = 0.0 · 2.45 = 0.0 KN-m/m

Strip load = $\sum$Lat factor $\cdot\, \gamma^2 \cdot Q/h \cdot [\beta$–sin $\beta^3 \cdot$ cos $(2\alpha)] = 1.60 \cdot 0.0 = 0.0$ KN/mArm = 0.00 m Moment = 0.0 · 0.00 = 0.0 KN-m/m

Wind load $= WL\ factor \cdot Pressure \cdot Wind\ height = 0.0 \cdot 0.00 \cdot 1.52 = 0.0$ KN/mArm = Stem – Wind height / 2 = 2.60 – 1.52 / 2 = 1.84 m Moment = 0.0 · 1.84 = 0.0 KN-m/m

Backfill seismic $= EQ\ factor \cdot (P_{aeh}–P_{ah}) = 0.0 \cdot (36.8–36.8) = 0.0$ KN/mArm = 0.6 · Hb = 0.6 · 2.60 = 1.56 m Moment = 0.0 · 1.56 = 0.0 KN-m/m

Water seismic $= EQ\ factor \cdot P_{we} = 0.0 \cdot 0.0 = 0.0$ KN/m

Arm = (Water table – Ftg) / 3 = (2.30 – 0.3 / 100) / 3 = 0.77 m Moment = 0.0 · 0.77 = 0.0 KN-m/m **Wall seismic** = 0.0 KN/m Moment = 0.0 KN-m/m

Maximum values Max. shear = 58.8 + 14.1 + 0.0 + 0.0 + 0.0 + 0.0 + 0.0 = 72.9 KN/m

Max. moment = 51.0 + 9.4 + 0.0 + 0.0 + 0.0 + 0.0 + 0.0 = 60.4 KN-m/m

Shear strength $\phi V_n = 0.11 \cdot \phi \cdot (\sqrt{f_c})^2 \cdot 10 \cdot Thick \cdot 100 \phi V_n = 0.11 \cdot 0.60 \cdot (22)^{1/2} \cdot 10 \cdot 0.90 \cdot 100 = 279.9$ KN/m $>$ 72.9 KN/mOKACI Table 14.5.5.1

Shear friction $\phi V_n = \phi \cdot \mu \cdot 1.2 \cdot Stem\ Weight \phi V_n = 0.75 \cdot 1.00 \cdot 1.2 \cdot 37.4 = 33.7$ KN/m $<$ 72.9 KN/mNG ACI 22.9.4.5

Bending strength $\phi M_n = 0.42 \cdot \phi \cdot \sqrt{f_c} \cdot L \cdot Thick^2/6$

Top: $\phi M_n = 0.42 \cdot 0.60 \cdot \sqrt{22} \cdot 100 \cdot 30.02/6/100/10 = 17.8$ KN-m/m

Bottom: $\phi M_n = 0.42 \cdot 0.60 \cdot \sqrt{22} \cdot 100 \cdot 90.02/6/100/10 = 160.3$ KN-m/m $>$ 60.4 KN-m/m$\color{red}{OK}$

ACI 14.5.2.1

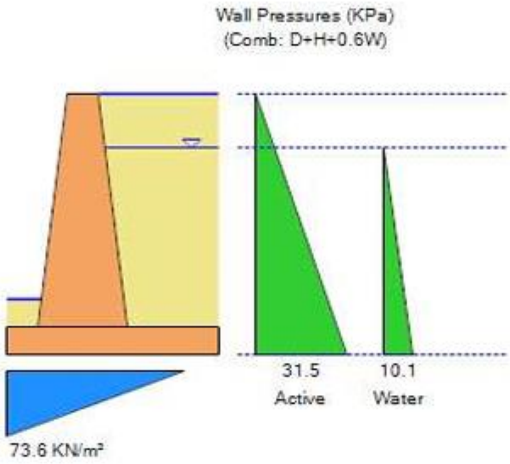

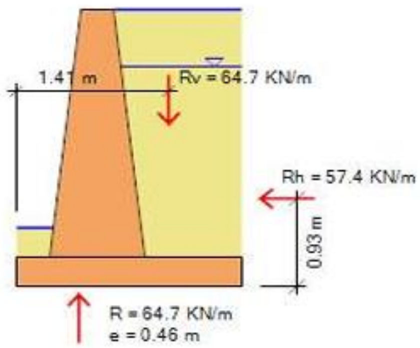

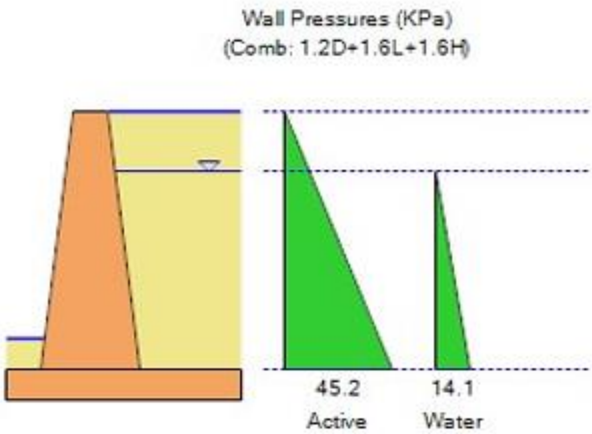

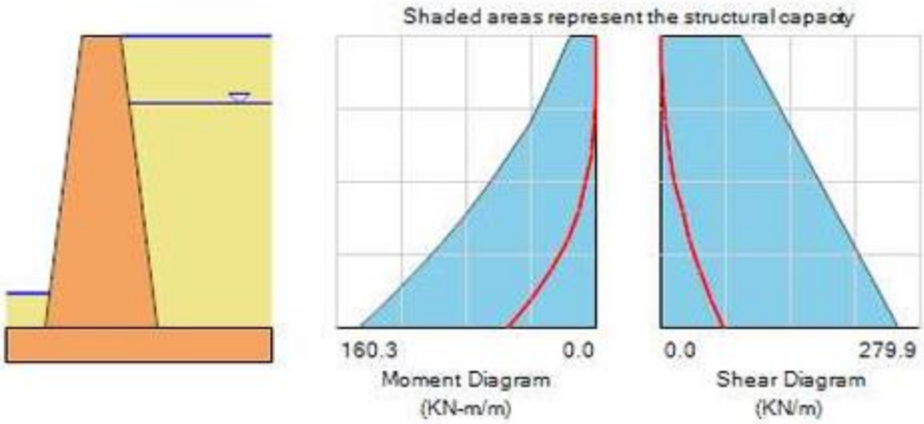

HEEL DESIGN (Comb. 1.4D + 0.9H)

Bearing force = 0.0 KN/m (Neglect bearing pressure for heel design) Arm = N.A. Moment = 0.0 KN-m/m

Concrete weight $= DL\ factor \cdot Thick \cdot Heel \cdot \gamma_c = 1.40 \cdot 0.30 \cdot 0.90 \cdot 24.00 = 9.1$ KN/mArm = Heel / 2 = 0.90 / 2 = 0.45 m Moment = 9.1 · 0.45 = 4.1 KN-m/m

Backfill weight $= DL\ factor \cdot Heel \cdot Height \cdot \gamma = 1.40 \cdot 0.90 \cdot 2.60 \cdot 16.5 = 54.1$ KN/mArm = Heel / 2 = 0.90 / 2 = 0.45 m Moment = 54.1 · 0.45 = 24.3 KN-m/m

Backfill slope $= DL\ factor \cdot (Heel \cdot \Delta Thick) \cdot Wedge/2 \cdot \gamma = 1.40 \cdot (0.90 \cdot 0.30 \cdot 0.00/2 \cdot 16.5) = 0.0$ KN/mArm = Heel · 2 / 3 = 0.90 · 2 / 3 = 0.60 m Moment = 0.0 · 0.60 = 0.0 KN-m/m

Water $= Factor \cdot Heel \cdot (Water\ table–Fig) \cdot (\gamma_s–\gamma) = 1.40 \cdot 0.90 \cdot (2.30–0.30) \cdot (18.3–16.5) = 4.5$ KN/mArm = Heel / 2 = 0.90 / 2 = 0.45 m Moment = 4.5 · 0.45 = 2.0 KN-m/m

Surcharge $= Srch\ factor \cdot (Heel \cdot \Delta Thick) \cdot Surcharge = (1.40 \cdot 0.00 \cdot 0.00) \cdot (0.90 + 0.30) = 0.0$ KN/mArm = Heel / 2 = 0.90 / 2 = 0.45 m Moment = 0.0 · 0.45 = 0.0 KN-m/m

Max. Shear V_u= –0.0 + 9.1 + 54.1 + 0.0 + 4.5 + 0.0 = 67.7 KN/m

Max. Moment M_u= –0.0 + 4.1 + 24.3 + 0.0 + 2.0 + 0.0 = 30.4 KN-m/m

Shear strength $\phi V_n = 0.11 \cdot \phi \cdot \sqrt{f_c'} \cdot 10 \cdot Thick \cdot 100 \phi V_n = 0.11 \cdot 0.66 \cdot \sqrt{25} \cdot 10 \cdot 0.30 \cdot 100 = 279.9$ KN/m > 72.9 KN/mOKACI Table 14.5.5.1

Bending strength $\phi M_n = 0.42 \cdot \phi \cdot f_c' \cdot L \cdot Thick^2/6 \phi M_n = 0.42 \cdot 0.66 \cdot \sqrt{22} \cdot 100 \cdot 0.30^2/6/100 = 18.9$ KN-m/m < 30.4 KN-m/mNG ACI 14.5.2.1

TOE DESIGN (Comb. 0.9D + 1.6H + W)

Bearing force $= (Bearing_1 + Bearing_2)/2 \cdot Toe = (249.1 + 106.2)/2 \cdot 0.30 = 53.3$ KN/m

$$\text{Arm} = \frac{Bearing_1 \cdot Toe^2/2 + (Bearing_2 - Bearing_1) \cdot Toe^2/3}{Force} = \frac{106.2 \cdot 0.30^2/2 + (249.1 - 106.2) \cdot 0.30^2/3}{53.3} = 0.17 \text{ m}$$

Moment = 53.3 · 0.17 = 9.1 KN-m/m

Water Buoyancy $= Factor \cdot \gamma_w \cdot Water\ table \cdot Toe = 0.9 \cdot 9.8 \cdot 2.30 \cdot 0.30 = 6.1$ KN/mArm = Toe / 2 = 0.30 / 2 = 0.15 m Moment = 6.1 · 0.15 = 0.9 KN-m/m

Concrete weight $= DL\ factor \cdot Thick \cdot Toe \cdot \gamma_c = 0.9 \cdot 0.30 \cdot 0.30 \cdot 24.00 = 1.9$ KN/m

Arm = Toe / 2 = 0.30 / 2 = 0.15 m Moment = 1.9 · 0.15 = 0.3 KN-m/m

Soil cover $= DL\ factor \cdot Toe \cdot Height \cdot \gamma = 0.9 \cdot 0.30 \cdot 1.49 \cdot 16.5 = 1.3$ KN/mArm = Toe / 2 = 0.30 / 2 = 0.15 m Moment = 1.3 · 0.15 = 0.2 KN-m/m

Max. Shear V_u= 53.3 + 6.1 – 1.9 – 1.3 = 56.1 KN/m

Shear at critical section $V_u = Max\ shear \cdot (Toe–d)/Toe = 56.1 \cdot (0.30–21.4/100)/0.30 = 16.0$ KN/m

Max. Moment M_u= 9.1 + 0.9 – 0.3 – 0.2 = 9.5 KN-m/m

Shear strength $\phi V_n = 0.11 \cdot \phi \cdot \sqrt{f_c'} \cdot 10 \cdot Thick \cdot 100 \phi V_n = 0.11 \cdot 0.66 \cdot \sqrt{25} \cdot 10 \cdot 0.30 \cdot 100 = 279.9$ KN/m > 72.9 KN/mOKACI Table 14.5.5.1

Bending strength $\phi M_n = 0.42 \cdot \phi \cdot \sqrt{f_c'} \cdot L \cdot Thick^2/6 \phi M_n = 0.42 \cdot 0.66 \cdot \sqrt{22} \cdot 100 \cdot 30.0^2/6/100/10 = 18.9$ KN-m/m > 9.5 KN-m/mOKACI 14.5.2.1

DESIGN CODESs

General Analysis: IBC 2021

Concrete Design: ACI 318-19

Load Combinations: ASCE 7-16/22

MATERIALS

Concrete f_c'(MPa): Stem = 22.2, Footing = 25.0

Rebars f_y(MPa): Footing = 7.0

Masonry f_m'(MPa): 10.3

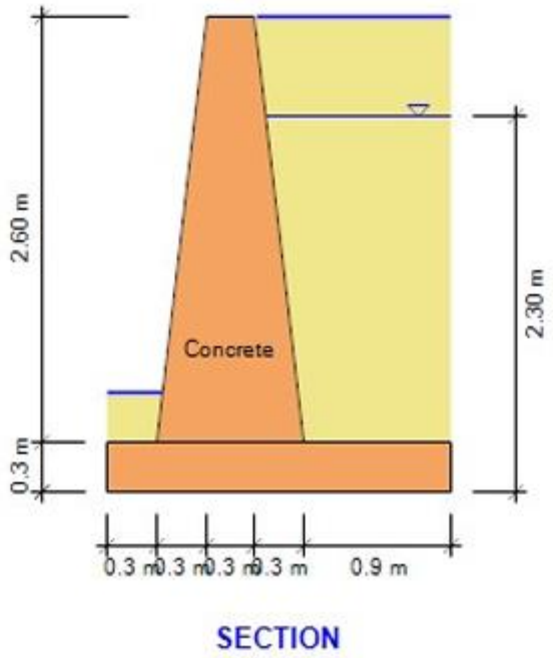

Table 8:The summary of stability factor of safety of the current status of the retaining wall

Stability factor of safety	
Overturning	1.71 > 1.5
Sliding	0.64 < 1.5
Bearing capacity	0.87 < 1.0

Analysis of the Current Stability Status.

From table 8, The initial assessment of the existing wall yielded a sliding Factor of Safety (FoS) of 0.64 and a bearing capacity of 0.87. These results represent a critical failure state. Recent research by (Das and Sobhan, 2021) highlights that soils with internal friction angles as low as 11° typical of saturated alluvial deposits cannot provide sufficient frictional resistance to balance active pressures without significant mechanical stabilization. The failure to meet the minimum FoS of 1.5 for sliding is consistent with findings by (Cheng and Lau, 2023), who argue that hydrostatic pressure in irrigation structures often acts as a "destabilizing catalyst" that reduces effective stress and triggers sliding.

4.3 Results for specific objective three (SO3)

To evaluate the robustness of the retaining wall design, several loading scenarios were simulated in ASDIP Retain.

Baseline Condition (Dry Condition)

To establish a reference point for the analysis, a Baseline Condition (Dry Condition) was modeled representing the current wall geometry under normal groundwater levels. This baseline configuration featured a concrete gravity retaining wall with a stem height of 3.40 m, tapering from a top thickness of 0.40 m to a base thickness of 1.40 m. The structural foundation comprised a 0.30 m thick footing with a 0.60 m toe and a 2.30 m heel, protected by a soil cover of 0.50 m at the toe. Geotechnically, the model utilized a backfill height of 3.40 m with a level slope (0.0°) and a foundation soil characterized by an internal friction angle of 11°.

The resulting stability analysis from ASDIP Retain indicated that the wall is structurally sound under these specific dry conditions. The Factor of Safety (FoS) against overturning was calculated at 5.04, well above the required 1.5 threshold, while the sliding resistance yielded a FoS of 1.52, successfully meeting the minimum 1.5 design limit. Additionally, the bearing capacity FoS reached 2.06, exceeding the required 1.0 limit. Consequently, the baseline results demonstrate that the structure maintains adequate stability during normal groundwater cycles before adverse hydraulic pressures are introduced.

Table 9:The baseline condition for factors of safeties

Stability factor of safety	
Overturning	5.04 > 1.5
Sliding	1.52 > 1.5
Bearing capacity	2.06 > 1.0

From the table above, all factor of safety passes for baseline condition.

Combined Adverse Condition

The Combined Adverse Condition represents the most critical, worst-case loading scenario for the retaining wall, characterized by the simultaneous impact of elevated groundwater levels and reduced soil shear strength. To ensure structural resilience under these extreme parameters, specifically maintaining an internal friction angle of 11° the wall geometry required significant modification. The optimized model for this scenario utilized a 3.40 m stem height (0.40 m top and 1.40 m bottom thickness) and an increased footing thickness of 0.60 m. Most notably, to counteract hydraulic uplift and lateral pressure, the heel length was extended to 4.70 m, while the toe length and soil cover were maintained at 0.60 m and 0.50 m, respectively, under a 3.40 m backfill.

The resulting stability analysis from ASDIP Retain confirmed that this " Dimensional Scaling" geometric adjustment successfully met all safety criteria. The Factor of Safety against overturning was calculated at 8.54, and the sliding resistance was brought to 1.52, both of which exceed the required 1.50 design threshold. Additionally, the bearing capacity yielded a Factor of Safety of 1.96, comfortably surpassing the 1.0 limit. While these results validate that the wall can remain stable under the most severe site conditions, the requirement for a massive 4.70 m heel suggests that relying solely on geometric expansion may be architecturally and economically inefficient compared to soil improvement strategies.

Table 10:The combined condition to check the stabilities.

Stability	Factor of safety
Overturning	8.54 > 1.5
Sliding	1.52 > 1.5
Bearing capacity	1.96 > 1

Discussion of Loading Scenarios (Tables 9 & 10)

The analysis of the "Combined Adverse Condition" revealed that under saturated conditions, the current soil parameters required an impractical heel length of 4.70 m to reach stability. This drastic increase in geometry illustrates the impact of hydraulic coupling.

(Vardhan and Kumar, 2022) noted that when the water table rises in the backfill, the resulting buoyancy forces can reduce the wall's effective resisting weight by up to 30%. In your model, the buoyancy force of 47.4 KN/m directly undermined the sliding resistance. As established by (Hovnanyan et al, 2023), designing for the "worst-case scenario" (saturated conditions) is now a standard requirement for resilient infrastructure rehabilitation to prevent the common failures seen in older gravity structures.

The table above shows that all stability factors pass at worst case scenario when the toe length is longer than the wall height. This is okay but however it's not cost effective and inefficient from the AASTHTO and ACI318, therefore the first 1m depth of first layer with internal angle of friction should be excavated and replaced with an improved material with better angle of internal friction.

The strategic over-excavation and replacement of the 1.0 m incompetent soil layer is consistent with the geotechnical improvement methodologies established by Das and (Sivakugan, 2018). This approach recognizes that substituting low-shear-strength surficial deposits with engineered granular fill significantly enhances both the ultimate bearing capacity and the sliding resistance at the foundation interface. By improving these fundamental soil-structure interaction parameters, the design migrates from a geometrically inefficient footprint to a highly optimized configuration. This methodology effectively eliminates the structural redundancies and excessive material costs associated with the previous 4.70 m heel length, demonstrating that localized ground improvement is a superior alternative to oversized reinforced concrete elements in achieving both safety and economic feasibility.

Optimized soil Replacement from 11^0 to 26^0

By utilizing the properties of the second soil layer, which offers an improved angle of internal friction of 26°, a more optimized and cost-effective structural design was achieved for the worst-case scenario. In this configuration, the wall dimensions were refined to a stem height of 3.40 m with a top thickness of 0.30 m and a bottom thickness of 1.10 m. The foundation was streamlined to a footing thickness of 0.40 m with a 0.60 m toe and a significantly reduced heel length of only 1.30 m, compared to the 4.70 m required in previous simulations. The soil cover at the toe was set at 0.40 m to protect the 3.40 m high backfill.

Excavation and Replacement of weak Foundation Soil

To improve the stability and bearing performance of the retaining wall foundation, the weak and weak upper soil layer should be excavated and replaced with compacted granular fill material. The excavation should be carried out to a uniform depth of 1.0 m along the entire length of the retaining wall. The retaining wall has a total length of 150 m, and excavation should be performed over a width of 2.0 m on each side of the wall foundation. The purpose of this soil replacement was to remove the weak foundation material that contributed to excessive settlement and instability, and to substitute it with an engineered granular material possessing improved shear strength characteristics with an internal friction angle of 26°.

The excavation volume was determined using the standard earthwork relationship

Excavation Volume = Depth × Length × Width

For one side of the retaining wall

$$V = 1.0 \times 150 \times 2.0 = 300\,m^3$$

Since excavation should be conducted on both sides of the retaining wall, the total excavation volume became

$$V_{total} = 300 \times 2 = 600\,m^3$$

Accordingly, a total of **600 m^3** of unsuitable soil was removed and replaced with compacted granular material to enhance the geotechnical performance and overall stability of the retaining wall system.

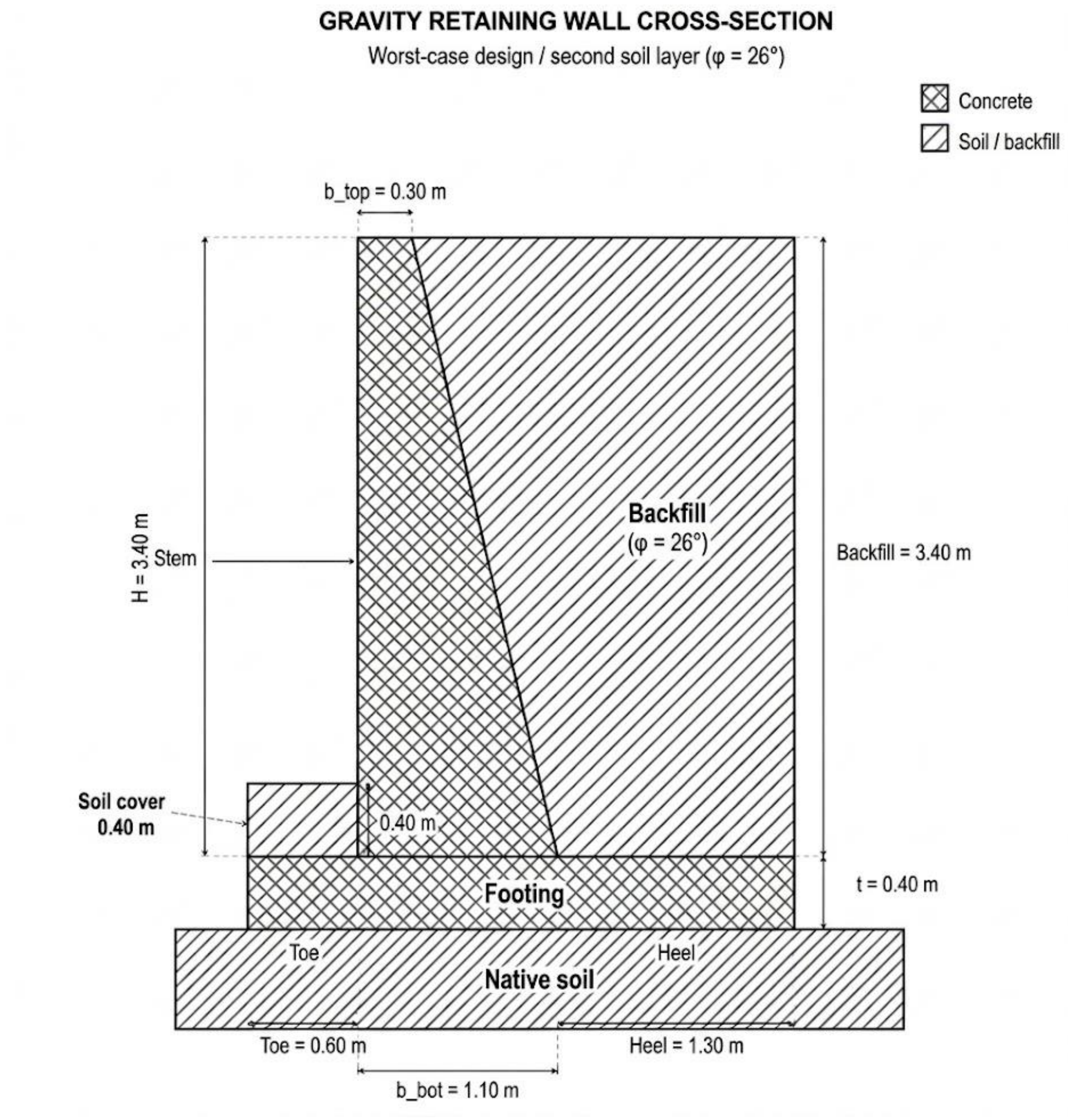

Figure 8:Cross section of gravity retaining wall geometry for optimized soil replacement.

The stability results for this optimized model demonstrate high efficiency while maintaining full safety compliance. The Factor of Safety against overturning was recorded at 3.67, comfortably exceeding the 1.5 threshold. The sliding stability was successfully maintained at 1.52, meeting the mandatory design limit, and the bearing capacity Factor of Safety was calculated at 1.6, which is well above the required 1.0 limit. This scenario confirms that soil replacement or improvement of the foundation layer allows for a much more practical and sustainable structural footprint without compromising the integrity of the retaining wall.

Table 11:The final result for the worst-case scenario of the better retaining wall.

Stability factor of safety	
Overturning	3.67 > 1.5
Sliding	1.52 > 1.5
Bearing capacity	1.6 > 1

4.3.1 Structural Modeling in ASDIP Retain

The structural modeling of the retaining wall was conducted using ASDIP Retain, adhering strictly to ACI 318 design provisions for gravity structures. The numerical model integrated comprehensive geometric and material parameters, including wall height, stem thickness, and base width, while accounting for concrete unit weight and critical soil properties such as cohesion (c) and the internal friction angle (ϕ).

To ensure the long-term integrity of the design, three primary stability checks were performed. First, the Factor of Safety against overturning was evaluated as the ratio of resisting moments to overturning moments (FSOT = M resisting / M overturning ≥ 1.5). The results across the three scenarios showed a high level of compliance. the baseline condition yielded a FoS of 5.04, which increased to 8.54 in the combined adverse condition due to the enlarged footing, and finally stabilized at an efficient 3.67 in the optimized third scenario. This final value comfortably exceeds the 1.5 design limit, demonstrating superior structural efficiency.

Secondly, sliding stability was assessed by comparing resisting forces comprised of friction (with an assumed coefficient $\mu = 0.45$) and passive soil resistance against the lateral driving forces from active earth pressure and surcharge. Across all three investigated conditions (Baseline, Combined Adverse, and Optimized Soil replacement), the sliding Factor of Safety was successfully maintained at 1.52. This consistent result confirms that the design meets the mandatory FoS ≥ 1.5 requirement, providing a robust defense against lateral displacement even under worst-case hydraulic loading.

Finally, bearing capacity stability was determined using the Terzaghi equation, which accounts for soil cohesion, foundation depth, and width to calculate the ultimate bearing capacity (qu). The software evaluated the allowable pressure against the applied pressure to ensure the foundation remains within safe limits. In the baseline condition, the bearing FoS was 2.06, which slightly decreased to 1.96 under combined adverse conditions. In the final optimized scenario utilizing an internal friction angle of 26°, the bearing capacity factor was 1.6. This value remains well above the 1.0 threshold, confirming that the foundation is capable of supporting the structure without the risk of shear failure or excessive settlement.

Table 12:The summary of whole factor of safety using ASDIP Retain.

Number	Condition	overturning factor of safety
1	Basiline condition at angle of internal friction 11 deg	5.04
2	Combined condition with the same angle of 11 deg	8.54
3	Combined condition of angle of intrarenal friction 26 deg	3.67

Number	Conditions	Sliding factor of safety
1	Basiline condition at angle of internal friction 11 deg	1.52
2	Combined condition with the same angle of 11 deg	1.52
3	Combined condition of angle of intrarenal friction 26 deg	1.52

Number	Condition	Bearing capacity
1	Basiline condition at angle of internal friction 11 deg	2.06 > 1.5
2	Combined condition with the same angle of 11 deg	1.96 > 1.5
3	Combined condition of angle of intrarenal friction 26 deg	1.6 > 1

Discussion of the result for table 11 and 12.

The final optimization utilized a soil replacement strategy, increasing the foundation friction angle to 26°. This resulted in an Overturning FoS of 3.67, a Sliding FoS of 1.52, and a Bearing Capacity FoS of 1.60.

This improvement demonstrates that the geotechnical properties of the foundation are more influential than the structural volume of the wall. (Wang et al, 2020) emphasize that for retaining walls on weak soil, soil replacement or "cushioning" is a superior rehabilitation strategy compared to concrete thickening, as it improves the interface friction coefficient. By reaching a sliding FoS of 1.52, the design now complies with the (ACI 318-19, 2019) and (IBC, 2021). Furthermore, the bearing capacity shift from 0.87 (failure) to 1.60 (pass) proves that the soil replacement effectively distributes the pressure bulb, a phenomenon documented by(Liu and Wang, 2022) in recent case studies of irrigation intake rehabilitations.

5 CHAPTER FIVE. CONCLUSIONS AND RECOMMENDATIONS

5.1 Conclusion.

The geotechnical and material assessment of the Doho Irrigation Scheme intake leads to the following conclusions:

Specific objective One (SO1)

The foundation rests on a highly compressible subgrade with CBR values as low as 4% to 8%, indicating insufficient shear strength to support the intake's vertical and lateral loads. This represents a critical "geotechnical mismatch," as the internal friction angle of 11° and allowable bearing capacity of 35 kPa fall significantly below safety requirements. Furthermore, high plasticity and linear shrinkage (up to 15%) render the soil prone to destabilizing volume changes during irrigation cycles. While the concrete strength (22.2 MPa) is adequate for basic loads, it lacks the optimal density required for high-pressure hydraulic environments.

Specific objective Two (SO2)

The intake is in a critical failure state, with a sliding Factor of Safety of 0.64 and a bearing capacity of 0.87, both of which fall significantly below standard design safety thresholds. Numerical validation confirms that this structural distress is driven by the foundation soil's failure to provide frictional resistance rather than a deficiency in construction materials. This instability is further exacerbated by perennial saturation, which exerts a buoyancy force of 47.4 kN/m a destabilizing catalyst that reduces effective stress and effectively halves the soil's resistance to sliding

Specific objective Three (SO3)

Stability analysis demonstrates that while the wall is safe under dry conditions, it fails immediately upon the introduction of adverse hydraulic pressures. Attempting to stabilize the structure through "Dimensional Scaling" requires an impractical heel length of 4.70 m, proving that geometric expansion alone is cost-ineffective and architecturally inefficient. Consequently, the assessment concludes that the most viable rehabilitation strategy is the strategic over-excavation of the weak 11° friction angle layer of $600\ m^3$ and its replacement with improved granular material to ensure long-term structural resilience.

5.2 Recommendations

To ensure the long-term stability and resilience of the Doho Irrigation Scheme intake, the following measures are recommended:

Seepage Analysis. A dedicated seepage study should be conducted to model the flow nets around the intake structure to prevent future scour at the toe.

Periodic Monitoring. Settlement gauges and tiltmeters should be installed post-rehabilitation to monitor the structure's performance during peak flooding seasons.

REFERENCES.

AASHTO. (n.d.). *American Association of State Highway and Transportation Officials. (2022). Standard method of test for the California Bearing Ratio (AASHTO T 193)*.

Abbas et al. (2020). *Abbas, M. F., et al. (2020). Geotechnical properties and swelling potential of high plasticity clays. International Journal of Geo-Engineering*.

ACI 318-19. (2019). No Title. *ACI (American Concrete Institute). (2019). Building Code Requirements for Structural Concrete (ACI 318-19) and Commentary*.

ASDIP Structural Software. (2023). *ASDIP Structural Software. (2023). ASDIP Retain User's Manual.*

ASTM International. (2018). No Title. *ASTM D6951/D6951M–18: Standard Test Method for Use of the Dynamic Cone Penetrometer in Shallow Pavement Applications.*

Avery. (2025). *oho Rice Irrigation Scheme in Uganda. Journal of Irrigation and Drainage Engineering*.

Bhattacharjee and Gunda. (2021). *Bhattacharjee, S., & Gunda, S. K. (2021). Correlation between linear shrinkage and mineralogical properties of expansive soils. Journal of Earth System Science*.

British Standards. (2022). *British Standards Institution. (2022). Methods of test for soils for civil engineering purposes. Classification tests and determination of water content, density and particle density (BS 1377-2:2022). BSI.*

BS EN. (2023). *Eurocode 2: Design of concrete structures. General rules and rules for buildings. British Standards Institution.*

Bwambale, E. (2019). *Bwambale, E. (2019). Hydraulic performance evaluation of the water conveyance system of Doho Rice Irrigation Scheme in Uganda.*

Cheng and Lau. (2023). No Title. *Cheng, Y. M., & Lau, C. K. (2023). Slope Stability Analysis and Stabilization: New Methods and Insight (3rd Ed.). Routledge*.

Clayton et al. (2014). *Clayton, C. R. I., Milititsky, J., & Woods, R. I. (2014). Earth Pressure and Earth-Retaining Structures (3rd ed.). CRC Press.*

Dalinghaus Construction. (2024a). *Dalinghaus Construction. (2024). What Causes Retaining Walls to Fail? Retrieved from https://www.dalinghausconstruction.com/blog/what-causes-retaining-*

walls-to-fail.

Dalinghaus Construction. (2024b). *What Causes Retaining Walls to Fail? Retrieved from https://www.dalinghausconstruction.com/blog/what-causes-retaining-walls-to-fail*.

Das & Sobhan. (2018). *Das, B. M., & Sobhan, K. (2018). Principles of Geotechnical Engineering (9th ed.). Cengage Learning.*

Das and Sobhan. (2013). No Title. *Das, B. M., & Sobhan, K. (2013). Principles of Geotechnical Engineering. Cengage Learning. (Used for CBR Classification).*

Das and Sobhan. (2021). No Title. *Das, B. M., & Sobhan, K. (2021). Principles of Geotechnical Engineering. 10th Ed. Cengage Learning. (Provides the Most Recent Standards for CBR and Soil Strength Classification).*

Done, S., & Samuel, P. (2004). *UK DCP 2.2 - User Manual: Measurement of Road Pavement Strength by Dynamic Cone Penetrometer*.

Eze et al. (2024). *Eze, K. N., Anosike, C. U., Eze, F. N., Enabulele, E. C., & Benson, K. P. (2024). Climate resilient and sustainable infrastructures: Geotechnical challenges of problematic soils in Nigeria. Civil and Environmental Engineering Reports, 34, 521–538.*

Garcia, A. R., Filipe, S. B., Fernandes, C., Estevão, C., & Ramos, G. (n.d.).

Geoengineer.org et al. (2020). *Geoengineer.org. (2020). Retaining Wall Collapse in Manistee Riverwalk, Michigan. Retrieved from https://www.geoengineer.org/news/retaining-wall-collapse-in-manistee-riverwalk-michigan*.

Hovnanyan et al. (2023). No Title. *Hovnanyan, A., Pimentel, K., & Soroushian, P. (2023). Resilience-Based Design of Retaining Structures under Extreme Hydraulic Conditions. Journal of Infrastructure Preservation and Resilience, 4(1), 12-25.*

IBC. (2021). No Title. *Nternational Code Council. (2021). 2021 International Building Code (IBC).*

Ituka, G. (2022). *Ituka, G. (2022). Impacts of Doho Rice Irrigation Scheme on water quality and wetland services in eastern Uganda.*

Jones and Smith. (2020). No Title. *Jones, R., & Smith, T. (2020). Structural Assessment of Small-Scale Irrigation Infrastructure. Journal of Rural Engineering. (Used for Comparative Failure Causes).*

Jp uganda aids Pdf et el. (2016). *Jp uganda aids Pdf*.

Khelalfa. (2025). *Khelalfa, H., Boulkhiout, F., & Kaikea, Y. (2025). Investigating the instability of a retaining wall: Construction concerns and design revisions. Romanian Journal of Civil Engineering*.

Kim. (2025). *Kim, M. (2025). Field DCP testing, MSEW analysis, and monitoring-based investigation of a reinforced earth retaining wall collapse.*

Li et al. (2025). *Li, F., Zhang, L., & Wang, H. (2025). Stability analysis and sustainable cutoff wall parametric optimization. Sustainability, 17(8), 3736. https://doi.org/10.3390/su17083736*.

Liu and Wang. (2022). No Title. *Liu, X., & Wang, H. (2022). Optimization of Gravity Retaining Walls through Soil Replacement: A Comparative Numerical Study. Geotechnical and Geological Engineering*.

Makhlouf et al. (2025). *Makhlouf, A. A., Elbeltagi, A., & El-Refaie, M. (2025). Lahoun regulator wing wall failure and a rehabilitation strategy. Springer Geotechnical Engineering, 10(1), 1981. https://doi.org/10.1007/s41062-025-01981-4*.

Ministry of works. (2000). *Ministry of Works. (2000). Laboratory testing manual. Central Materials Laboratory, United Republic of Tanzania.*

Muthler Landscaping. (2024). *Muthler Landscaping. (2024). Why Retaining Walls Fail - How To Build One Correctly. Retrieved from https://muthlerlandscaping.com/articles/why-retaining-walls-fail*.

Ng et al. (2019). *Ng, C. W. W., et al. (2019). Effects of wetting and drying cycles on the shear strength of unsaturated soils. Géotechnique*.

P, N. D. (2013). Uganda Vision 2040. *Annual Meeting of the Midwest Political Science …*, *12*(3), 1–7. http://web.stanford.edu/class/e297a/Neo-Colonialism in Africa.pdf%0Ahttps://eeas.europa.eu/sites/eeas/files/uganda-fr-forprint-14-04-2016_en_0.pdf%0Ahttps://reliefweb.int/sites/reliefweb.int/files/resources/85C0E269BAF5E780C12577B300447BAD-Full_Report.pdf

Pietroiusti et al. (2023). *Pietroiusti, R., Vanderkelen, I., Otto, F. E. L., Barnes, C., Temple, L., Akurut, M., Bally, P., van Lipzig, N. P. M., & Thiery, W. (2023). Possible role of anthropogenic climate change in the record-breaking 2020 Lake Victoria levels and floods. Copernic*.

Rutajama, M. S. S. (2000). Laboratory Testing Manual 2000. *Laboratory Testing Manual, Central Materials Laboratory- Tanzania*, pp 1-320.

RWPS LLC et al. (2024). *RWPS LLC. (2024). St. Louis Retaining Walls Fail Without Drainage – Here's Why. Retrieved from https://rwpsllc.com/why-retaining-walls-fail-st-louis-drainage-problems-explained/.*

Sadek et al. (2023). No Title. *Sadek, S., et Al. (2023). "Impact of Seepage on the Stability of Small-Scale Hydraulic Structures." Journal of Geotechnical and Geoenvironmental Engineering. (Directly Relates to the "Wet" Conditions at Your Irrigation Site).*

Sazzad and Islam. (2021). No Title. *Sazzad, M. S., & Islam, M. R. (2021). Comparative Study of Slope Stability and Retaining Wall Analysis Using Various Software Tools. Journal of Soft Computing in Civil Engineering*.

Sivakugan. (2018). *Das, B. M., & Sivakugan, N. (2018). Principles of Foundation Engineering (9th ed.). Cengage Learning.*

Sivakumar et al. (2015). No Title. *Sivakumar, V., et Al. (2015). The Effect of Saturation on the Shear Strength of Unsaturated Soils. Geotechnical and Geological Engineering. (Used to Explain the "Wet" Moisture Results).*

Stonehenge Brick Paving and Landscaping. (2024). *Stonehenge Brick Paving and Landscaping. (2024). 5 Reasons Your Retaining Wall Failed. Retrieved from https://stonehengebpl.com/5-reasons-your-retaining-wall-failed*.

Tiza et al. (2021). *Tiza, M., et al. (2021). Evaluation of California Bearing Ratio (CBR) of soils for irrigation infrastructure foundations. Journal of Engineering Research and Reports*.

Vardhan and Kumar. (2022). No Title. *Vardhan, H., & Kumar, J. (2022). Seismic and Hydraulic Coupled Stability of Retaining Walls: A Review of Recent Advancements. Geotechnical Engineering Journal of the SEAGS & AGSSEA*.

Varga et al. (2024). *Varga, R., Žlender, B., & Jelušič, P. (2024). Optimization of embedded retaining walls under the effects of groundwater seepage using a reliability-based and partial factor design approach. Applied Sciences, 14(23), 11135. https://doi.org/10.3390/app14231*.

Varghese. (2021). No Title. *Varghese, P. C. (2024). Foundation Engineering. 2nd Ed. PHI Learning. (Discusses the Local Shear Failure Mechanisms Identified in Your Ministry of Works Report).*

Wamala et al. (2023). *Wamala, F., Gidudu, A., Wanyama, J., Nakawuka, P., Bwambale, E., & Chukalla, A. D. (2023). Assessment of irrigation water distribution using remotely sensed indicators: A case study of Doho Rice Irrigation Scheme, Uganda.*

Wang et al. (2020). No Title. *Wang, L., Zhang, G., & Li, X. (2020). Soil-Structure Interaction and Drainage Effects on the Stability of Retaining Walls. Modern Civil Engineering, 12(4), 334-348.*

Zhang et al. (2020). No Title. *Zhang, Y., et Al. (2020). "Influence of Water Content on the Shear Strength of Silty Clay." Advances in Civil Engineering. (Explains Why Your Wet-Site CBR and Friction Angles Are so Low).*

APPENDIX


Tuesday, February 24, 2026 14:01:47
0°20'15.308"N 32°38'13.233"E ±4.84m
307° NW
Central Materials Laboratory Kireka
Ministry of Works and Transport
Prime Radio
Kireka


MoWT


CONSTRUCTION
&
SUPERVISION TEAM

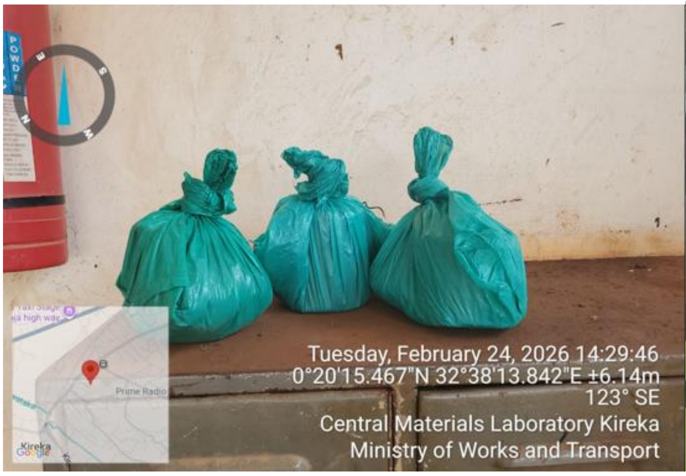
Tuesday, February 24, 2026 14:29:46
0°20'15.467"N 32°38'13.842"E ±6.14m
123° SE
Central Materials Laboratory Kireka
Ministry of Works and Transport